Soil Dynamics and Earthquake Engineering **12** (1993) 239–257

Dynamic response of pile groups with different configurations

George Gazetas, Ke Fan & Amir Kaynia

82 N. Kazantzaki St, Zografou 15772, Greece

(Received and accepted 10 November 1992)

A general methodology is outlined for a complete seismic soil–pile-foundation–structure interaction analysis. A Beam-on-Dynamic-Winkler-Foundation (BDWF) simplified model and a Green's-function-based rigorous method are utilized in determining the dynamic response of single piles and pile groups. The simplified model is validated through comparisons with the rigorous method. A comprehensive parameter study is then performed on the effect of pile group configuration on the dynamic impedances of pile foundations. Insight is gained into the nature of dynamic pile–soil–pile interaction. The results presented herein may be used in practice as a guide in obtaining the dynamic stiffness and damping of foundations with a large number of piles.

INTRODUCTION AND GENERAL METHODOLOGY

Seismic soil–pile-foundation–structure interaction analysis can be conveniently performed in three consecutive steps, as illustrated schematically in Figs 1–3:

(1) Obtain the motion of the foundation in the absence of superstructure inertia. This so-called *foundation input motion* includes translational as well as rotational components.
(2) Determine the dynamic impedances (*springs* and *dashpots*) associated with swaying (K_x or K_y), rocking (K_{ry} and K_{rx}) and cross-swaying–rocking (K_{x-ry} or K_{y-rx}) oscillations of the pile top.
(3) Compute the seismic response of the superstructure, supported on the *springs* and *dashpots* of step 2 and subjected at its base to the foundation input motion of step 1.

For each step of the analysis several alternative formulations have been developed and published in the literature, including finite-element formulations, boundary-element, semi-analytical and analytical solutions, and a variety of simplified methods. Table 1 lists some of the available methods. Three specific multi-step methods for computing soil–pile-foundation–structure interaction analysis have been proposed[1] which make use of rigorous as well as simplified methods. This paper uses the methods shown bold-faced in Table 1.

The objective of this study is to investigate the effect of *group configuration* on dynamic impedances of pile foundations. The results presented may be utilized to obtain realistic estimates of dynamic impedances of large pile groups embedded in homogeneous as well as in inhomogeneous soil profiles. This paper should be seen as a continuation of two previous publications by the authors and co-workers.[2,3]

SIMPLIFIED METHOD OF SOLUTION USED IN THIS PAPER

A Beam-on-Dynamic-Winkler-Foundation (BDWF) model developed by Gazetas and his co-workers has been used to determine the dynamic response of single piles and pile groups.[3–7] The soil is modeled as a Winkler-foundation resisting the (vertical or lateral) pile motion by continuously distributed frequency-dependent linear springs (k) and dashpots (c) along the pile length. $k + i\omega c$ constitutes the vertical or lateral local impedance of the Winkler foundation.

Frequency-dependent values are assigned to these uniformly distributed spring and dashpot coefficients using the following algebraic expressions, developed by matching the dynamic pile-head displacements from Winkler and finite-element analyses.

$$k_z \approx 0{\cdot}6E_s(1 + \tfrac{1}{2}\sqrt{a_0}) \quad (1)$$

Soil Dynamics and Earthquake Engineering 0267-7261/93/$06.00

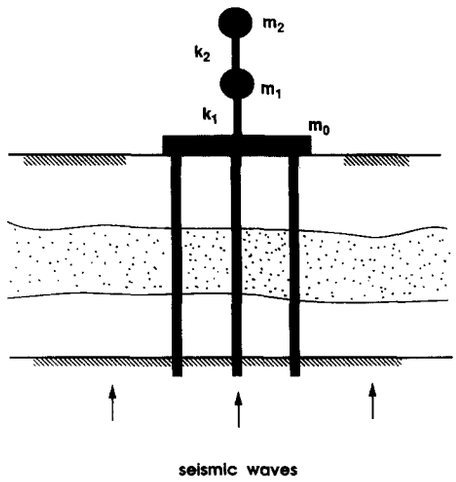

Fig. 1. Seismic soil–pile-foundation–structure interaction: the whole system.

$$c_z \approx 2\beta_s \frac{k_z}{\omega} + a_0^{-1/4} \rho_s V_s d \tag{2}$$

$$k_x \approx 1{\cdot}2E_s \tag{3}$$

$$c_x \approx 2\beta_s \frac{k_x}{\omega} + 6\rho_s V_s d(a_0)^{-1/4} \tag{4}$$

in which E_s is the Young's modulus, ρ_s is the mass density, β_s is the hysteretic damping and V_s is the shear wave velocity of the soil. Note that the unit of k_x is stiffness per unit length of the pile ($[F][L]^{-2}$) and the traditional subgrade modulus is in units of $[F][L]^{-3}$.

Similar k_x and c_x values can be obtained by Novak's plane strain elastodynamic solution for a rod oscillating in a continuum.[8–10] Novak's results would be exact for an infinitely long-and-rigid rod fully embedded in a

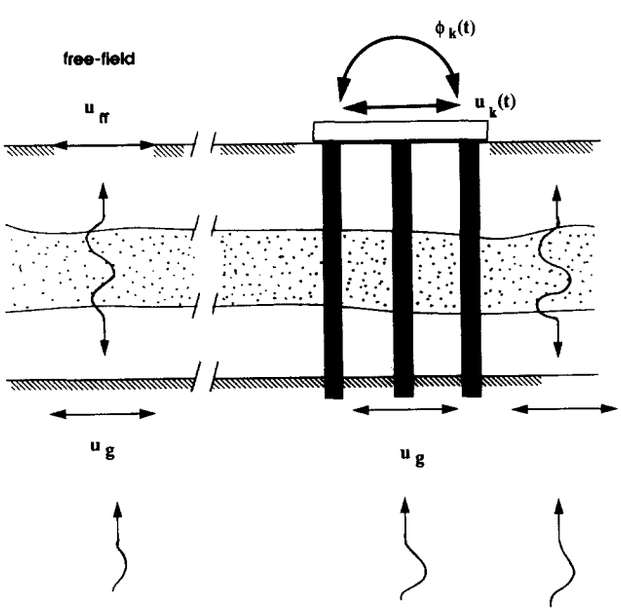

Fig. 2. Seismic soil–pile–foundation–structure interaction: kinematic seismic response analysis.

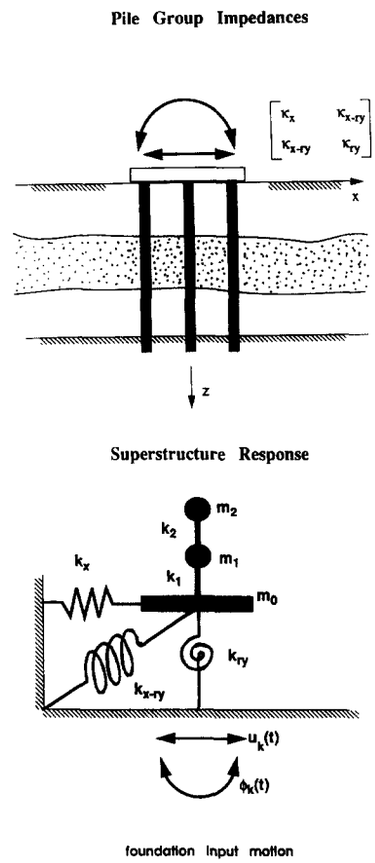

Fig. 3. Seismic soil–pile-foundation–structure interaction: inertial response analyses.

continuum space. By contrast, the expressions given above for radiation damping are derived in two steps:

(1) their form is first determined from a simple one-dimensional 'cone' model[11–13] which resembles Novak's model, but which, in contrast, *does* allow for some non-zero vertical deformation of the soil during lateral motion, as is appropriate due to the presence of the stress-free surface and to the non-uniformity with depth of pile deflections;
(2) the numerical coefficients of the expressions are then calibrated by essentially curve-fitting rigorous finite-element results, for a variety of pile–soil geometries and properties, as well as for different loading conditions.

The spring constants, on the other hand, are derived solely through curve-fitting, i.e. by matching pile-head stiffness of the Winkler and the finite-element formulations. One of the approximations introduced in deriving these equations is to neglect the (relatively small) influence of pile slenderness and flexibility (measured through L/d and E_p/E_s).

The resulting values of k_x and c_x from these equations at various frequencies are generally comparable with those of Novak. The expressions are preferred for three reasons. First, they are quite simple (since they do not

Table 1. General methodology for seismic soil–pile-foundation–structure interaction

1 DETERMINATION OF KINEMATIC SEISMIC RESPONSE
- **(a) Free-field (site) response**
  - One-dimensional elastic or inelastic wave propagation theories
  - Two- and three-dimensional elastic wave propagation theories
- **(b) Single pile response**
  - Beam-on-Dynamic-Winkler-Foundation (BDWF) model
  - Extended-Tajimi formulation
  - Finite-element formulations
  - Semi-analytical and boundary-element-type formulations
- **(c) Pile group response**
  - Simplified wave-transmission model
  - Extended-Tajimi formulation
  - Semi-analytical and boundary-element-type formulations

2 DETERMINATION OF PILE-HEAD IMPEDANCES
- **(a) Single pile**
  - Simple expressions
  - Extended-Tajimi formulation
  - BDWF model
  - Novak's plane-strain formulation
  - Novak–Nogami's axisymmetry formulation
  - Finite-element formulations
  - Semi-analytical and boundary-element-type formulations
- **(b) Pile group**
  - Superposition method (using dynamic interaction factors)
  - Extended-Tajimi formulation
- Finite-element formulation
- Other simplified solutions
- Semi-analytical and boundary-element-type formulations

3. DETERMINATION OF SUPERSTRUCTURE SEISMIC RESPONSE
- Must account for SSI through frequency-dependent foundation 'springs' and 'dashpots' from step 2 and must use the seismic response from step 1 as foundation excitation.

involve the rather complicated expressions with Bessel functions of complex argument of the Novak plane-strain solution). Second, they avoid the substantial underestimation of stiffness and overestimation of damping values by the plane-strain model at frequencies $\omega d/V_s < 1$, i.e. in the range of practical interest (Novak compensates for the underestimation in stiffness and overestimation in damping through empirical adjustments, which assume constant k_x and c_x below two different cut-off frequencies). Third, the lateral radiation damping expression does not exhibit the spurious high sensitivity to Poisson's ratio observed in the plane-strain Novak's solution, and which stems mainly from the restriction of vertical soil deformation.

It is also worth noting that dynamic Winkler springs and dashpots have been derived by Liou & Penzien, Roesset & Angelides and Kagawa & Kraft using yet another methodology.[14–16] They all utilized three-dimensional formulations (based either on Mindlin's static solution or on finite-element modeling) to relate local unit soil reaction to local pile deflection at various depths along the pile; a single complex-valued dynamic stiffness, S_z or S_x, to be uniformly distributed as springs and dashpots along the pile (as is appropriate for a Winkler foundation), was then derived by a suitable integration of local stiffnesses over depth. Only a limited number of results, pertaining to a uniform soil stratum, have been presented in those studies.

All the foregoing alternative methods give k and c values that are in reasonable accord for the range of frequencies of interest. Individual differences in the Winkler parameters usually do not exceed 10–20%.

The k_x and c_x values obtained from eqns (3) and (4) apply in real-life situations for frequencies ω above the stratum cut-off frequency. The latter is nearly identical with the natural frequency, $\omega_s = \pi V_s/2H_s$ in horizontal (shear) vibrations of the soil stratum. For $\omega < \omega_s$ radiation damping is vanishingly small, as a function of the material damping. One may then state:

$$c_x = (c_x)_{\text{hysteresis}} \approx 2\beta \frac{k_x}{\omega} \tag{5}$$

Similarly, the k_z and c_z expressions apply only for frequencies above the stratum cut-off frequency in vertical compression–extension vibration; this is approximately given by $\omega_c = 3{\cdot}4\omega_s/\pi(1-\nu_s)$.

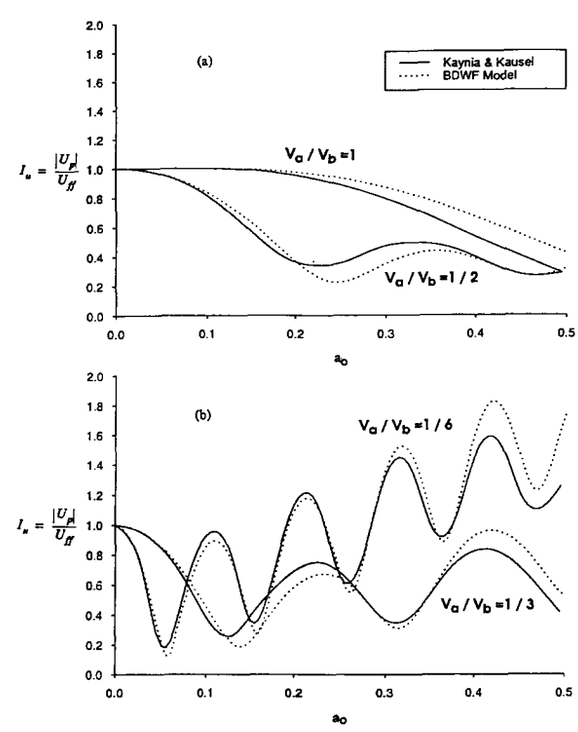

Fig. 4. Kinematic seismic response of fixed-head single pile: (a) $V_a/V_b = 1$, 1/2 and (b) $V_a/V_b = 1/3$, 1/6 ($E_p/E_{sb} = 1000$, $h_a = 5d$, $L/d = 20$, $\nu_s = 0{\cdot}4$, $\beta_s = 0{\cdot}05$).

For $\omega < \omega_c$,

$$c_z = (c_z)_{\text{hysteresis}} = 2\beta \frac{k_z}{\omega} \tag{6}$$

VALIDATION OF THE SIMPLIFIED METHOD

In order to verify the simplified method of solution utilized in this paper, the following selected comparisons, with results from rigorous solutions as well as from other simplified methods, are presented.

Figure 4 shows the kinematic displacement factor I_u of a single pile embedded in a two-layered stratum as a function of $a_0 = \omega d/V_s$, for a number of V_a/V_b ratios, obtained by the simplified method. V_a and V_b are the shear wave velocities of the upper and lower layers respectively. The thickness of the upper layer is one-quarter of the pile length. The same quantity evaluated by the boundary integral type of formulation[17] is also shown in the figure, which shows that the results from the simplified method agree extremely well with those of Kaynia & Kausel[17] for both homogeneous and two-layered deposits. An exception to the *general shape* of I_u versus a_0 is observed in Fig. 4(b). It refers to a soil deposit containing a thin, soft top layer ($h_a/d \leq 5$ and $V_a/V_b < 1.3$). As V_a/V_b decreases, i.e. as the top layer becomes relatively softer, the kinematic displacement factor tends to fluctuate with frequency at an increasing rate. At certain frequencies, the pile-head deflection may even be greater than the free-field surface displacement. The reason is that the pile cannot follow the ground motion within this upper layer when the velocity contrast between the two layers is large (e.g. $V_a/V_b = 1/6$).

The simplified method also gives encouraging results for the kinematic seismic response of pile groups. Figure 5 compares the kinematic displacement factor I_u of a 1×2 fixed-head pile group from the simplified and the rigorous methods. Notice that the differences are significant only for very stiff piles relative to the soil ($E_p/E_s = 10\,000$).

The dynamic impedances of a fixed-head single pile obtained from the BDWF model are displayed in Figs 6–8 and compared with the rigorous results (the impedances are normalized with the Young's modulus of the deposit). Evidently, the comparison between the corresponding swaying and cross-coupling impedances is very satisfactory. A minor discrepancy is observed between the rocking stiffnesses, but the damping terms match fairly well. Figure 9 compares the stiffness and damping computed by the two methods for a 2×2 pile group. Two pile spacing ratios ($s/d = 5$ and 10) are considered. The group stiffnesses and damping factors are in a good agreement.

The seismic response analysis of the complete soil–pile–foundation-structure system using the simplified method has been compared with the extended-Tajimi theory (see Ref. 18) and the results have been presented.[4,5] The two methods agree very well, although the extended-Tajimi method slightly overestimates the dynamic stiffness compared with the simplified method.

Therefore, it can be concluded that the simplified method of solution is satisfactory for both kinematic and inertial seismic response analyses.

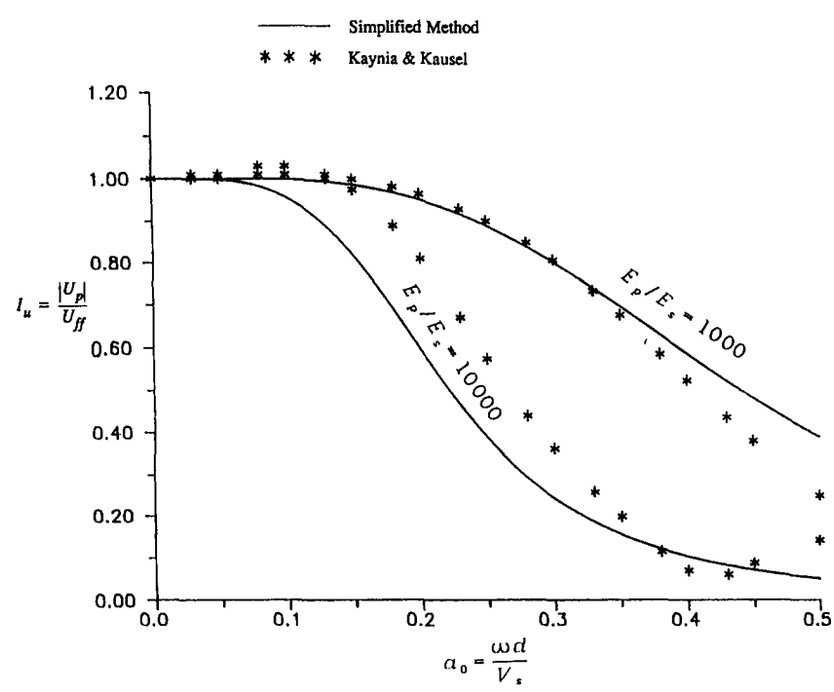

Fig. 5. Kinematic seismic response of a fixed-head 1×2 pile group.

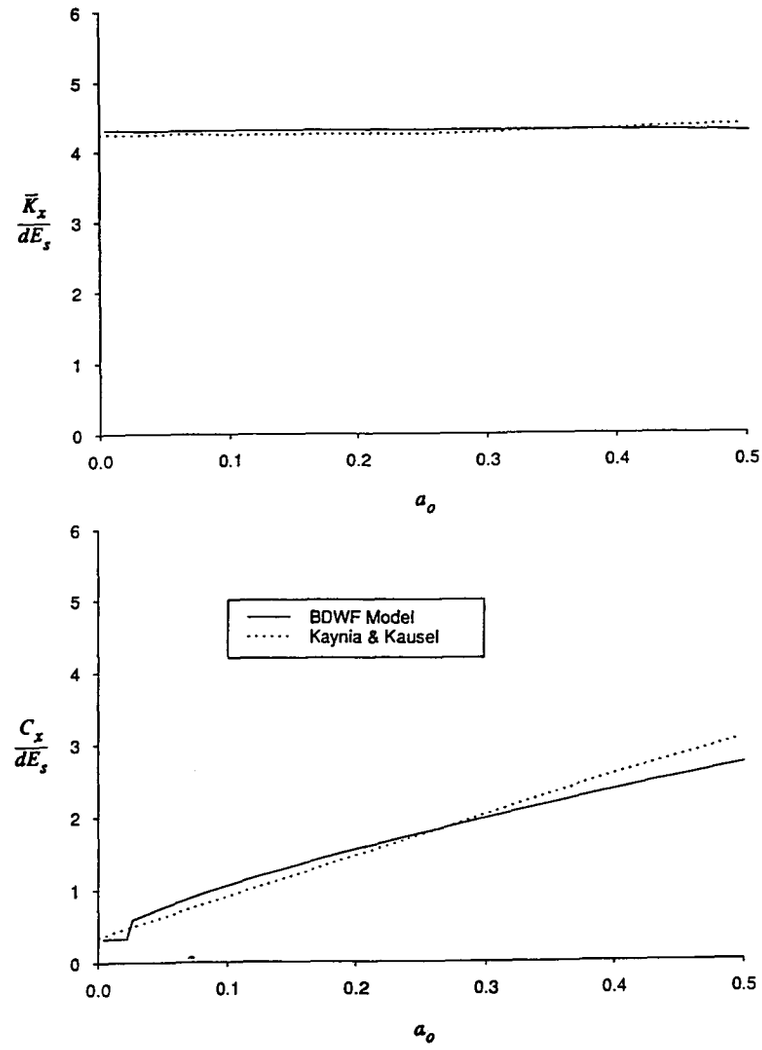

Fig. 6. Horizontal impedance of a single pile: comparison with the rigorous solution ($E_p/E_s = 1000$, $\rho_p/\rho_s = 1{\cdot}4$, $\nu_s = 0{\cdot}4$, $\beta_s = 0{\cdot}05$, $L/d = 20$).

EFFECT OF GROUP CONFIGURATION ON DYNAMIC IMPEDANCES OF PILE FOUNDATIONS IN SOFT SOIL

The major goal of this section is to investigate the influence of pile group configuration on dynamic impedances. Special attention is paid to the effects of frequency, spacing, the nature of the soil profile, and the number of piles in the group. In current engineering practice dynamic impedances of pile groups are usually estimated by using the impedances of a single pile and accounting for the group effect by means of static interaction factors. The other objective of this section is to study the applicability of dynamic interaction factors through comparison with rigorous numerical solution.

Figure 10 shows pile group configurations and soil profiles to be studied. All piles, of diameter d and length L, are considered to be linear elastic beams with constant Young's modulus, E_p, and mass density, ρ_p. Two typical soil deposits are investigated whose Young's modulus: (a) is constant (E_s) and (b) is proportional to depth $[E_s(z) = E_s(L)z/L]$. In both cases the soil is assumed to be a linear hysteretic continuum with constant Poisson's ratio ν_s, constant material density ρ_s, and constant hysteretic damping β_s.

Three categories of groups of floating piles are studied:

(1) a rigidly-capped $1 \times n$ linear pile group consisting of 1, 2, 3, 4, 6 or 9 piles in one row;
(2) a rigidly-capped $2 \times n$ rectangular group of 2×2, 2×3, 2×4, 2×5, or 2×6 piles in two rows;
(3) a rigidly-capped $n \times n$ square group of 2×2, 3×3, 4×4, or 6×6 piles.

The pile group is subjected to harmonic excitation at

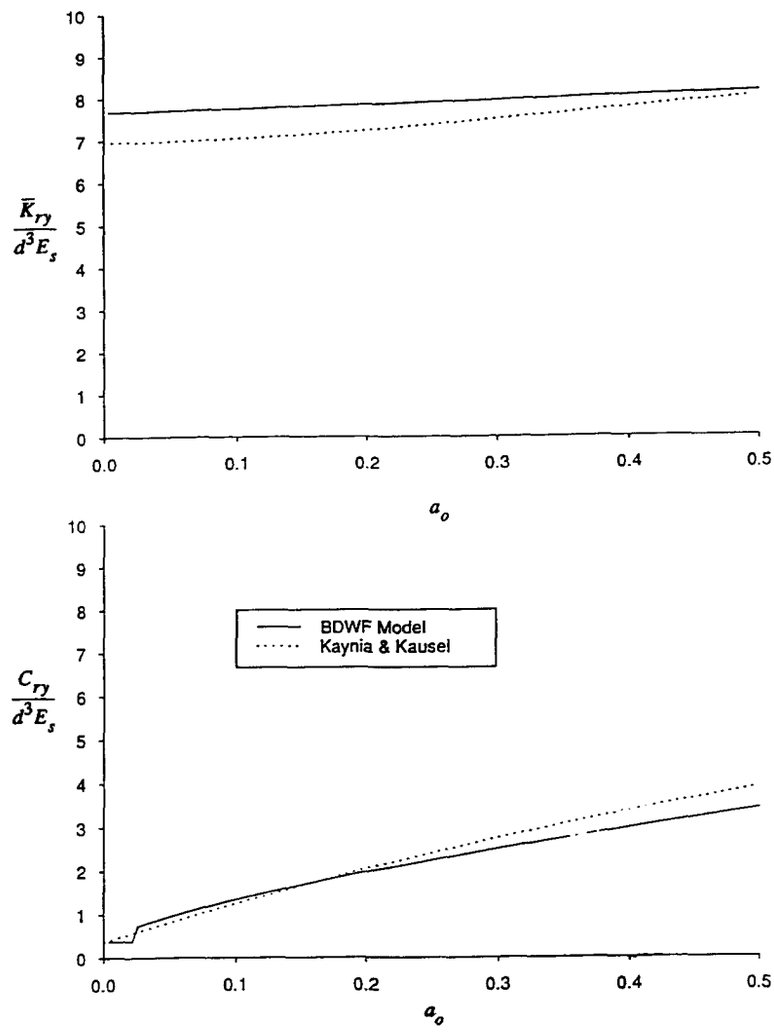

Fig. 7. Rocking impedance of a single pile: comparison with the rigorous solution ($E_p/E_s = 1000$, $\rho_p/\rho_s = 1{\cdot}4$, $\nu_s = 0{\cdot}4$, $\beta_s = 0{\cdot}05$, $L/d = 20$).

the top. The applied dynamic forces are transmitted onto each pile through a rigid cap. Vertical, horizontal, and rocking oscillations are considered. For each particular harmonic excitation of frequency ω, the complex-valued dynamic impedance κ of the group is defined as the ratio of total excitation (force F, or moment M) over the corresponding motion of rigid cap (displacement u, or rotation θ). In general, there are eight different impedances. Six of them correspond to the six possible modes of vibration of the pile head: vertical, κ_z; horizontal, κ_x and κ_y; torsional, κ_t; and rocking, κ_{rx} and κ_{ry}. Moreover, since horizontal forces along principal axes induce rotational in additional to translational oscillations, two more cross-coupling horizontal-rocking impedances exist: κ_{xry} and κ_{yrx}. Therefore, the 6×6 impedance matrix relating the force–movement vector $\{F_x, F_y, F_z, M_x, M_y, M_z\}^T$ with the displacement-rotation vector $\{u_x, u_y, u_z, \theta_x, \theta_y, \theta_z\}$ takes the form:

$$[\kappa] = \begin{bmatrix} \kappa_x & \kappa_{xry} & 0 & 0 & 0 & 0 \\ \kappa_{xry} & \kappa_{ry} & 0 & 0 & 0 & 0 \\ 0 & 0 & \kappa_y & \kappa_{yrx} & 0 & 0 \\ 0 & 0 & \kappa_{yrx} & \kappa_{rx} & 0 & 0 \\ 0 & 0 & 0 & 0 & \kappa_z & 0 \\ 0 & 0 & 0 & 0 & 0 & \kappa_t \end{bmatrix} \tag{7}$$

Presentation of parametric results

The impedances obtained by using the previous formulation are complex quantities and can be written as

$$\kappa = \bar{K} + \mathrm{i}\, a_0 \bar{C} \tag{8}$$

where $\bar{K}$ is the dynamic group stiffness, $\bar{C}$ is the group damping coefficient, which encompasses geometric and

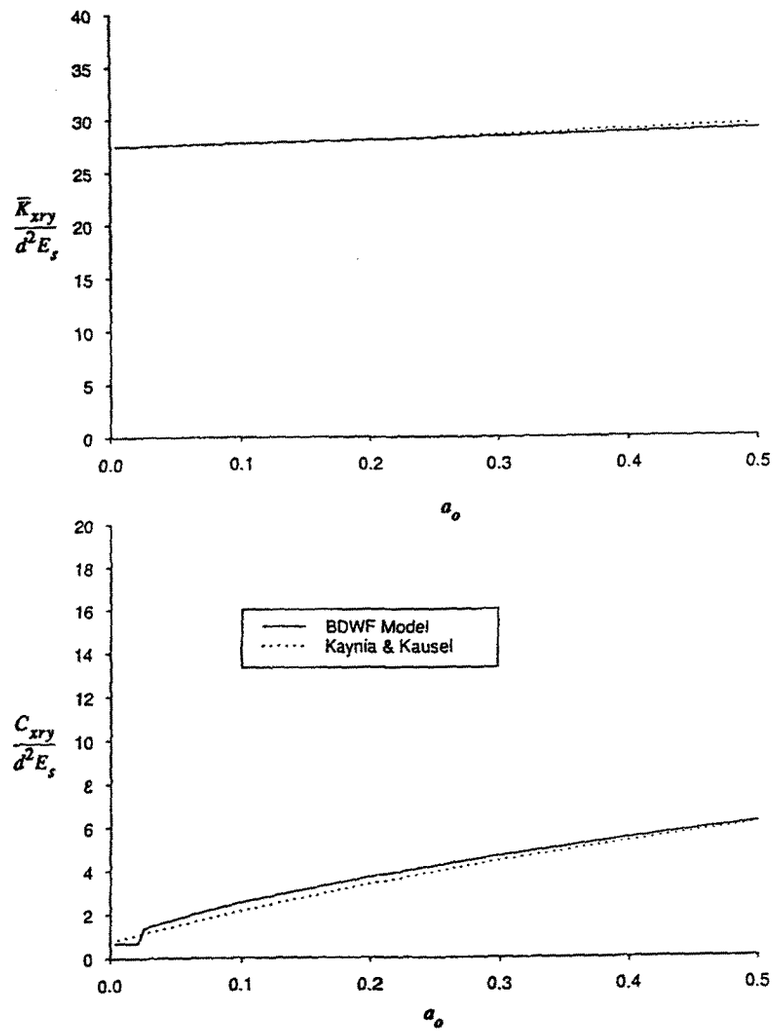

Fig. 8. Cross-coupling impedance of a single pile: comparison with the rigorous solution ($E_p/E_s = 1000$, $\rho_p/\rho_s = 1{\cdot}4$, $\nu_s = 0{\cdot}4$, $\beta_s = 0{\cdot}05$, $L/d = 20$).

hysteretic dissipation of energy, $a_0 = \omega d/V_s^*$ is dimensionless frequency and V_s^* is a characteristic value of the soil S-wave velocity profile (in this paper V_s^* is taken as equal to V_s for the homogeneous and to $V_s(L)$ for the nonhomogeneous profile).

Only vertical, horizontal and rotational impedances are given. Torsional and cross-coupling horizontal-rocking impedances will not be included here for lack of space. For vertical or horizontal oscillation, the dynamic impedance of the group is normalized with respect to the vertical or horizontal static stiffness of a single pile in the group ($K_z^{(1)}$ or $K_x^{(1)}$) multiplied by the number of piles, whereas for the rocking impedance both vertical and rocking static stiffness ($K_x^{(1)}$ and $K_{rx}^{(1)}$) of a single pile are used for normalization. Therefore, the 'dynamic stiffness group factor' $k^{(n)}$ and the 'damping group factor' $D^{(n)}$ are introduced as follows:

For vertical oscillation,

$$k_z^{(n)} = \frac{\bar{K}_z^{(n)}}{nK_z^{(1)}} \quad \text{and} \quad D_z^{(n)} = \frac{\bar{C}_z^{(n)}}{nK_z^{(1)}} \tag{9}$$

For horizontal oscillation,

$$k_x^{(n)} = \frac{\bar{K}_x^{(n)}}{nK_x^{(1)}} \quad \text{and} \quad D_x^{(n)} = \frac{\bar{C}_x^{(n)}}{nK_x^{(1)}}$$
$$k_y^{(n)} = \frac{\bar{K}_y^{(n)}}{nK_y^{(1)}} \quad \text{and} \quad D_y^{(n)} = \frac{\bar{C}_y^{(n)}}{nK_y^{(1)}} \tag{10}$$

For rocking oscillation,

$$k_{rx}^{(n)} = \frac{\bar{K}_{rx}^{(n)}}{nK_{rx}^{(1)} + \sum y^2 K_z^{(1)}} \quad \text{and} \quad D_{rx}^{(n)} = \frac{\bar{C}_{rx}^{(n)}}{nK_{rx}^{(1)} + \sum y^2 K_z^{(1)}}$$

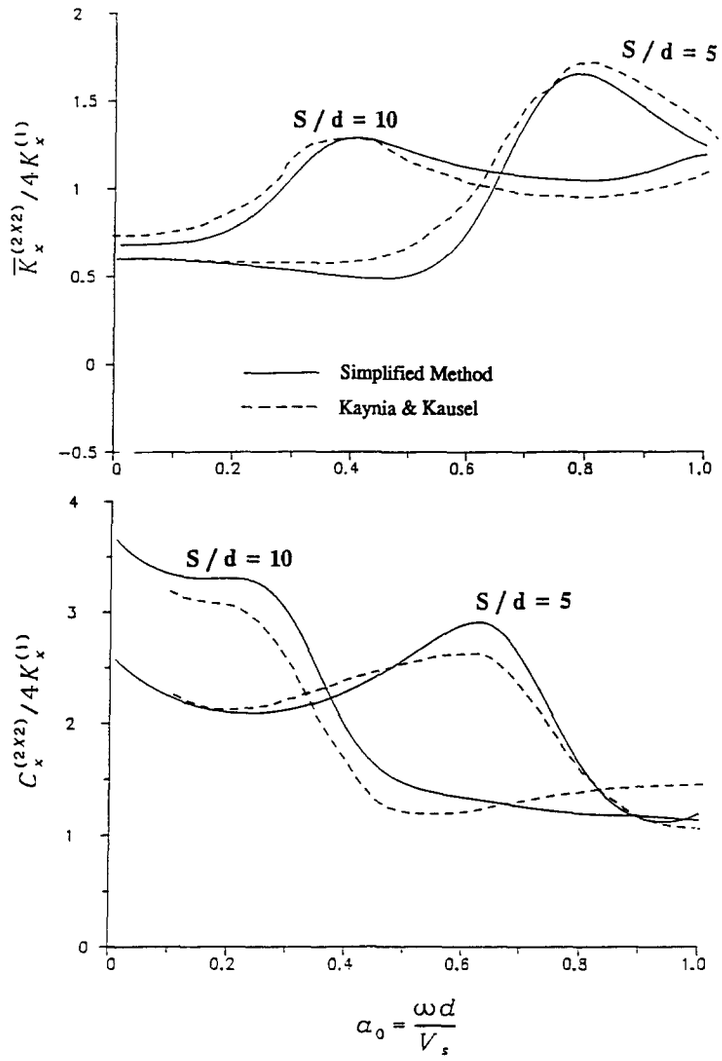

Fig. 9. Dynamic stiffness and damping group factors ($E_p/E_s = 1000$, $\rho_p/\rho_s = 1{\cdot}4$).

$$k_{ry}^{(n)} = \frac{\bar{K}_{ry}^{(n)}}{nK_{ry}^{(1)} + \sum x^2 K_z^{(1)}} \quad \text{and} \quad D_{ry}^{(n)} = \frac{\bar{C}_{ry}^{(n)}}{nK_{ry}^{(1)} + \sum x^2 K_z^{(1)}} \tag{11}$$

The stiffness and damping group factors are plotted according to the pile spacing ratio and configurations as follows: Figs 11–25 present results for linear groups of piles in a row, Figs 26–33 are for rectangular pile groups, and Figs 34–39 are for square pile groups.

Tables 2–5 present impedance functions of single pile and pile groups resulting from different methods, normalized by the Young's modulus E_s of the soil.

Analysis and discussion of results

The results presented here in figures and tables reveal the following significant trends.

An interesting common feature is that the group behavior (due to pile-to-pile interaction) is more pronounced as the number of piles increases. If there had been no interaction, the curves would have coincided with those of a single pile (broken lines) in which the stiffness deviates only slightly from unity in the frequency range considered. The radical change of group stiffness and damping takes place as the number of piles increases from one to two (Figs 16–25). In a linear group, increasing the number of piles beyond two or three has only a small effect on the dynamic stiffness and damping group factors, and the variation of the group stiffness and damping with frequency is fairly smooth. It is straightforward to explain this lack of strong interaction between piles in a linear group. Each new pile 'introduced' in an existing linear group would generate waves which would only affect the two or three nearest piles; when these waves are 180° out of phase with one of these piles, they are in phase with the next pile(s). As a result, the combined effect of wave interferences on impedances is quite small.

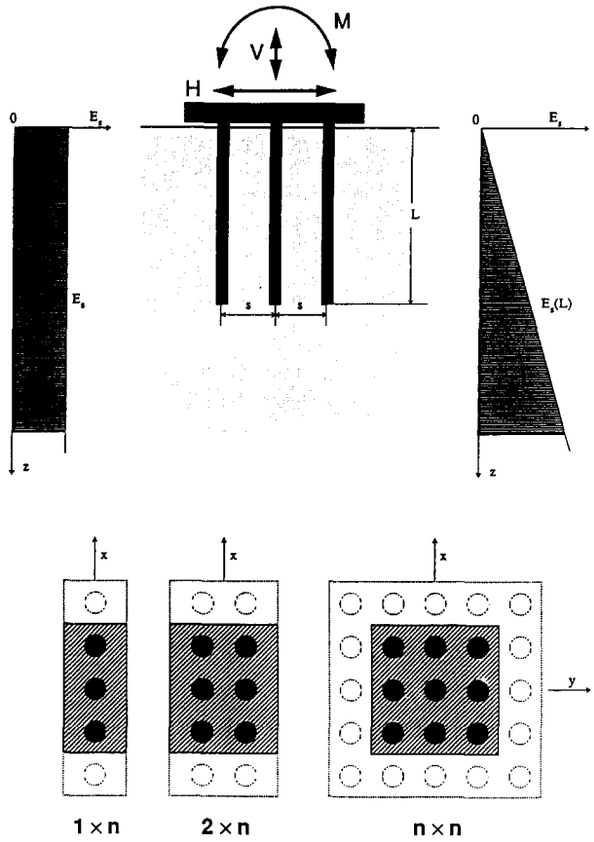

Fig. 10. Pile configurations and soil profiles studied.

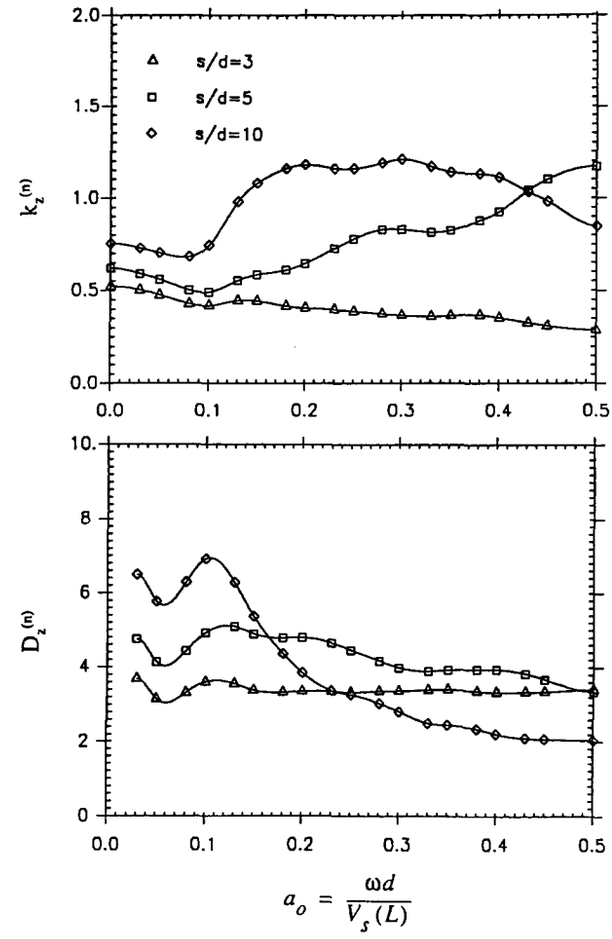

Fig. 11. Normalized vertical dynamic stiffness and damping group factors of 1×4 rigidly-capped pile groups in a nonhomogeneous half-space ($E_p/E_s(L) = 5000$, $L/d = 20$, $\rho_s/\rho_p = 0{\cdot}7$, $\beta_s = 0{\cdot}05$ and $\nu_s = 0{\cdot}4$): effects of frequency and pile separation distance.

By contrast, the interaction effect becomes increasingly pronounced as the number of rows in a pile group increases. Obviously, this is due to the pile-to-pile interaction between piles in opposite rows. Thus, peaks and valleys appear on the group stiffness and damping curves, which depend on the size of the group and the spacing of the piles. Figures 26–29 clearly show this transition of dynamic stiffness and damping group factors: smooth curves for the linear groups, fluctuating curves for rectangular and square pile groups. As a consequence, at certain frequencies the dynamic group efficiency may be much greater than unity. The only exception here is the rocking impedance κ_{rx} of $2 \times n$ pile groups. The explanation will be given in the subsequent paragraph.

For horizontal and rocking modes of oscillation in linear and rectangular pile groups, the group stiffness and damping in the x and y directions are, of course, different. As explained above, it is the interaction between piles in different rows that plays a dominant role in the dynamic response of pile groups. Therefore, the behavior of the group impedances κ_y and κ_{rx} is controlled by compression–extension waves emitted from the piles in one row or two rows, while the impedances κ_x and κ_{ry} are dominated by shear wave interferences. The rate of fluctuation of the group stiffness and damping is thus faster for κ_y and κ_{rx} than for κ_x and κ_{ry}. This is because compression–extension waves propagate at an apparent phase velocity $V \cong V_{La}$ ('Lysmer's analog' velocity), where $V_{La} = [3{\cdot}4/\pi(1-\nu_s)]V_s \cong 1{\cdot}8V_s$ (for $\nu_s = 0{\cdot}4$), leading to a faster fluctuation rate for κ_y and k_{rx}.

For rocking around the x-axis of the linear and rectangular pile groups (Figs 19, 24 and 32), the variation of the group stiffness and damping with frequency is very smooth. This is due to very small interaction taking place as a result of rotational deformation at the head of each pile in a row and because piles located on the opposite side of the x-axis oscillate axially 180° out of phase. However, the case of square pile groups is more complicated, and high peaks and valleys do appear on the curves.

In engineering practice, three approaches are used to obtain the dynamic impedances of pile groups: (a) the superposition method with use of static interaction factors, ignoring the frequency dependence of pile–pile interaction; (b) superposition with use of (simplified or

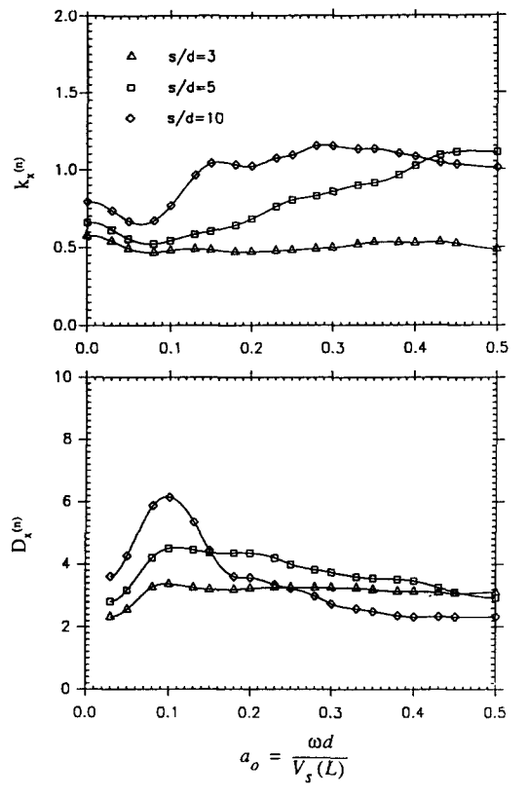

Fig. 12. Normalized horizontal dynamic stiffness and damping group factors of 1×4 rigidly-capped pile groups in a nonhomogeneous half-space ($E_p/E_s(L) = 5000$, $L/d = 20$, $\rho_s/\rho_p = 0{\cdot}7$, $\beta_s = 0{\cdot}05$ and $\nu_s = 0{\cdot}4$): effects of frequency and pile separation distance.

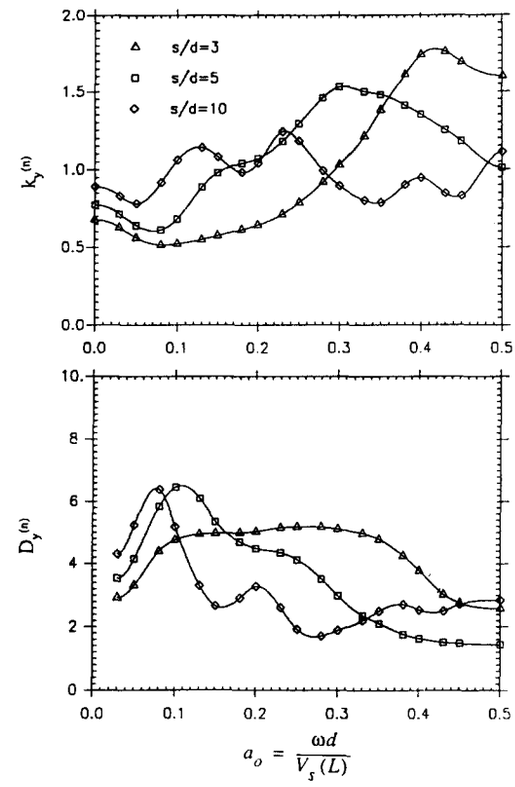

Fig. 13. Normalized horizontal dynamic stiffness and damping group factors of 1×4 rigidly-capped pile groups in a nonhomogeneous half-space ($E_p/E_s(L) = 5000$, $L/d = 20$, $\rho_s/\rho_p = 0{\cdot}7$, $\beta_s = 0{\cdot}05$ and $\nu_s = 0{\cdot}4$): effects of frequency and pile separation distance.

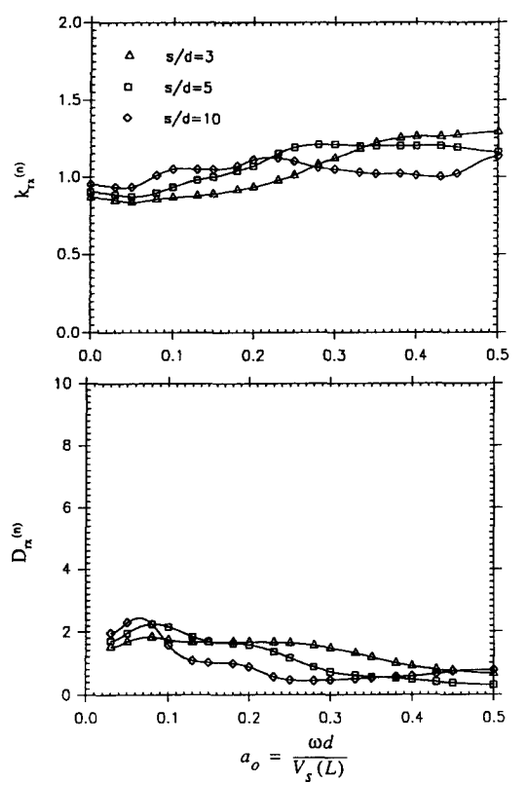

Fig. 14. Normalized rotational dynamic stiffness and damping group factors of 1×4 rigidly-capped pile groups in a nonhomogeneous half-space ($E_p/E_s(L) = 5000$, $L/d = 20$, $\rho_s/\rho_p = 0{\cdot}7$, $\beta_s = 0{\cdot}05$ and $\nu_s = 0{\cdot}4$): effects of frequency and pile separation distance.

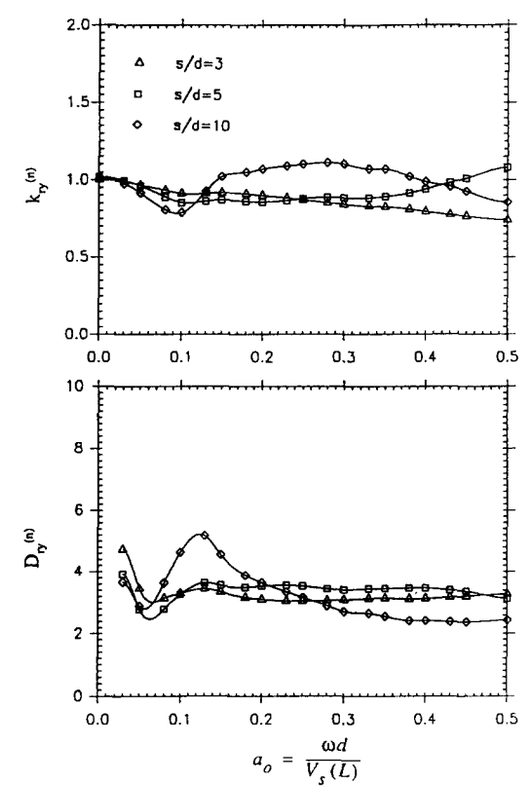

Fig. 15. Normalized rotational dynamic stiffness and damping group factors of 1×4 rigidly-capped pile groups in a nonhomogeneous half-space ($E_p/E_s(L) = 5000$, $L/d = 20$, $\rho_s/\rho_p = 0{\cdot}7$, $\beta_s = 0{\cdot}05$ and $\nu_s = 0{\cdot}4$): effects of frequency and pile separation distance.

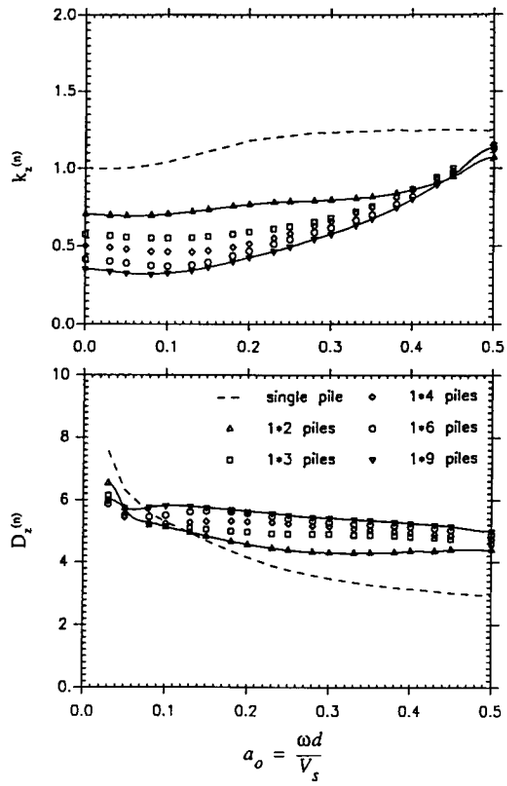

Fig. 16. Normalized vertical dynamic stiffness and damping group factors of $1 \times n$ rigidly-capped pile groups in a nonhomogeneous half-space ($E_p/E_s = 10\,000$, $L/d = 20$, $s/d = 5$, $\rho_s/\rho_p = 0{\cdot}7$, $\beta_s = 0{\cdot}05$ and $\nu_s = 0{\cdot}4$): effect of pile group configuration.

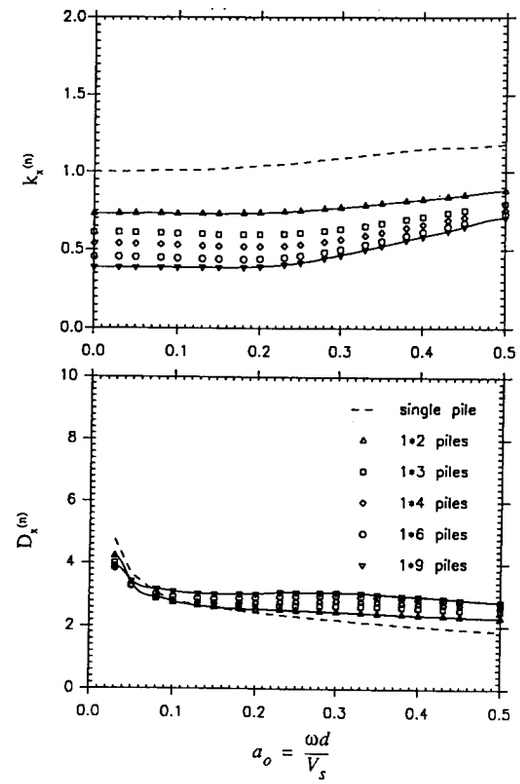

Fig. 17. Normalized vertical dynamic stiffness and damping group factors of $1 \times n$ rigidly-capped pile groups in a homogeneous half-space ($E_p/E_s = 10\,000$, $L/d = 20$, $s/d = 5$, $\rho_s/\rho_p = 0{\cdot}7$, $\beta_s = 0{\cdot}05$ and $\nu_s = 0{\cdot}4$): effect of pile group configurations.

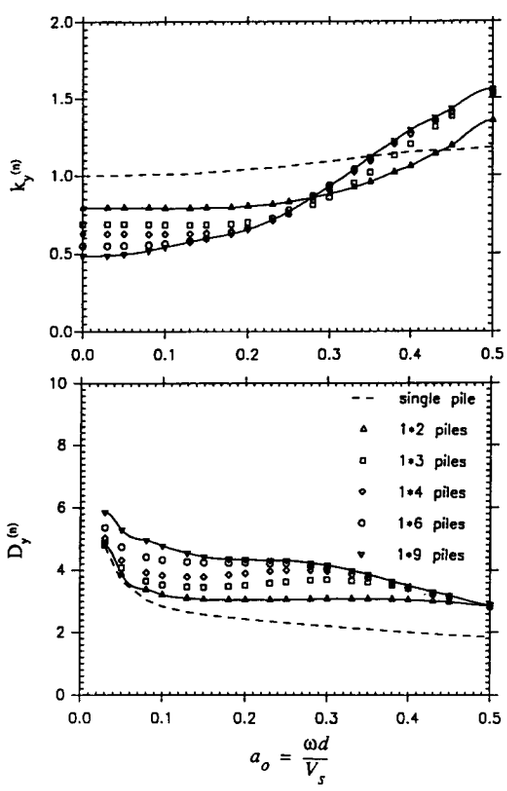

Fig. 18. Normalized horizontal dynamic stiffness and damping group factors of $1 \times n$ rigidly-capped pile groups in a homogeneous half-space ($E_p/E_s = 10\,000$, $L/d = 20$, $s/d = 5$, $\rho_s/\rho_p = 0{\cdot}7$, $\beta_s = 0{\cdot}05$ and $\nu_s = 0{\cdot}4$): effect of pile group configurations.

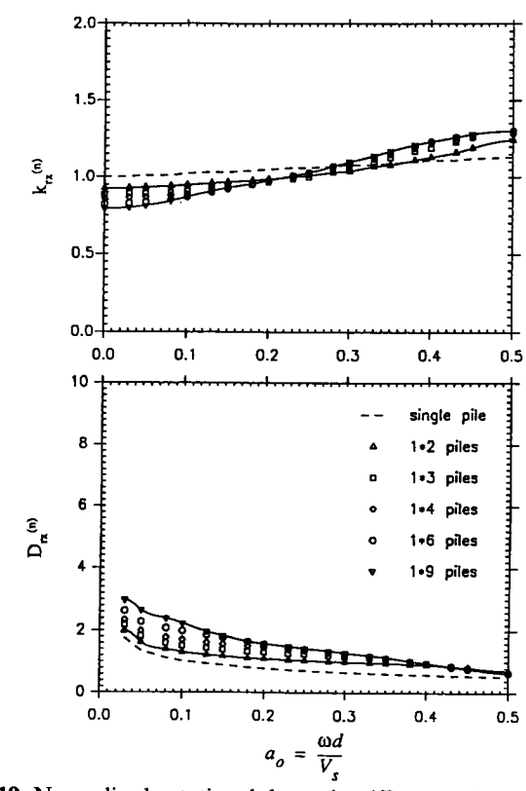

Fig. 19. Normalized rotational dynamic stiffness and damping group factors of $1 \times n$ rigidly-capped pile groups in a homogeneous half-space ($E_p/E_s = 10\,000$, $L/d = 20$, $s/d = 5$, $\rho_s/\rho_p = 0{\cdot}7$, $\beta_s = 0{\cdot}05$ and $\nu_s = 0{\cdot}4$): effect of pile group configurations.

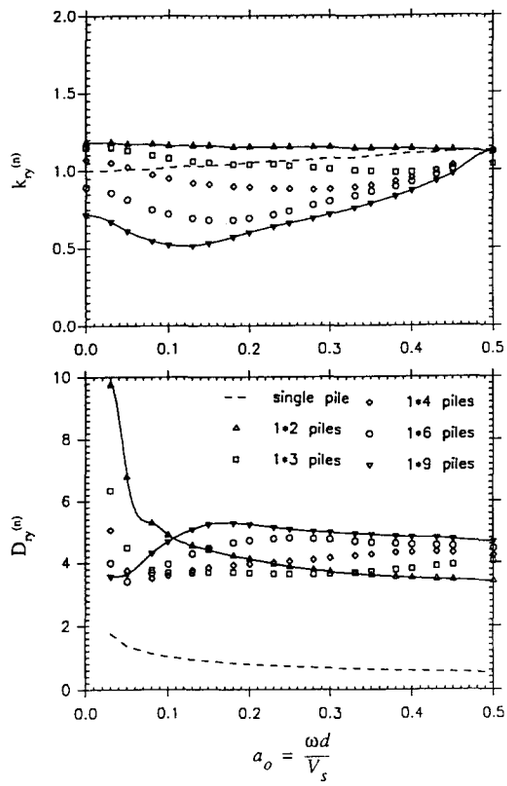

Fig. 20. Normalized rotational dynamic stiffness and damping group factors of $1 \times n$ rigidly-capped pile groups in a homogeneous half-space ($E_p/E_s = 10\,000$, $L/d = 20$, $s/d = 5$, $\rho_s/\rho_p = 0{\cdot}7$, $\beta_s = 0{\cdot}05$ and $\nu_s = 0{\cdot}4$): effect of pile group configurations.

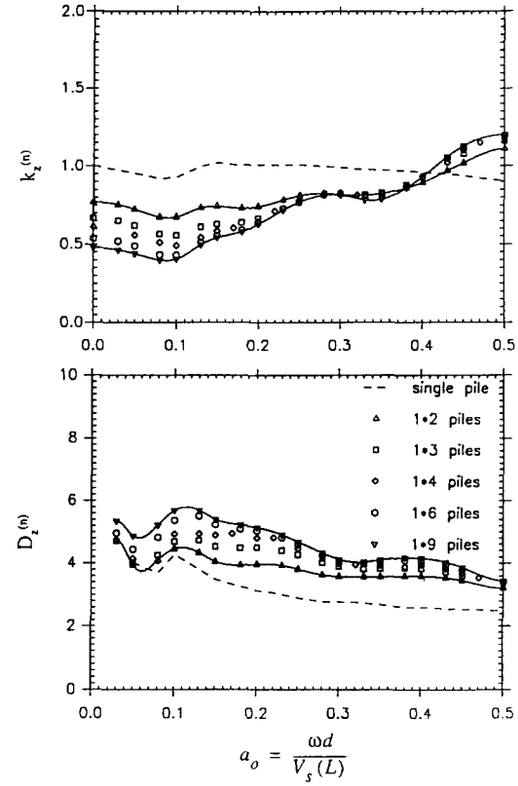

Fig. 21. Normalized vertical dynamic stiffness and damping group factors of $1 \times n$ rigidly-capped pile groups in a nonhomogeneous half-space ($E_p/E_s(L) = 5000$, $L/d = 20$, $s/d = 5$, $\rho_s/\rho_p = 0{\cdot}7$, $\beta_s = 0{\cdot}05$ and $\nu_s = 0{\cdot}4$): effect of pile group configurations.

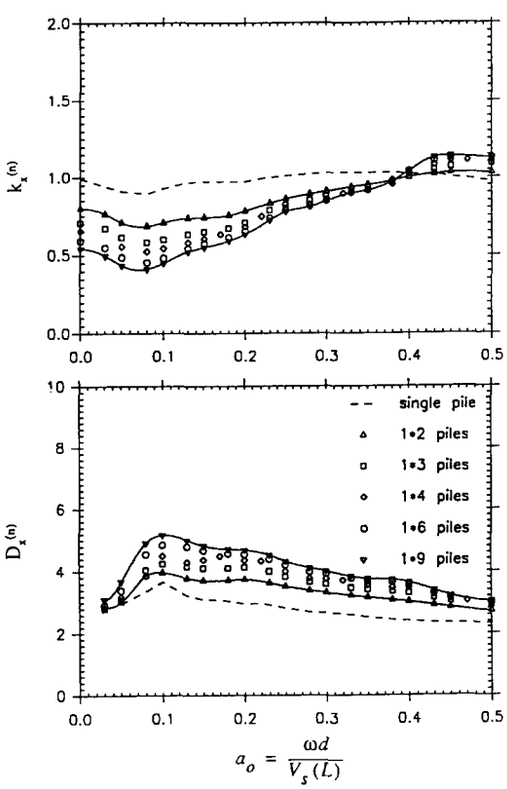

Fig. 22. Normalized horizontal dynamic stiffness and damping group factors of $1 \times n$ rigidly-capped pile groups in a nonhomogeneous half-space ($E_p/E_s(L) = 5000$, $L/d = 20$, $s/d = 5$, $\rho_s/\rho_p = 0{\cdot}7$, $\beta_s = 0{\cdot}05$ and $\nu_s = 0{\cdot}4$): effect of pile group configurations.

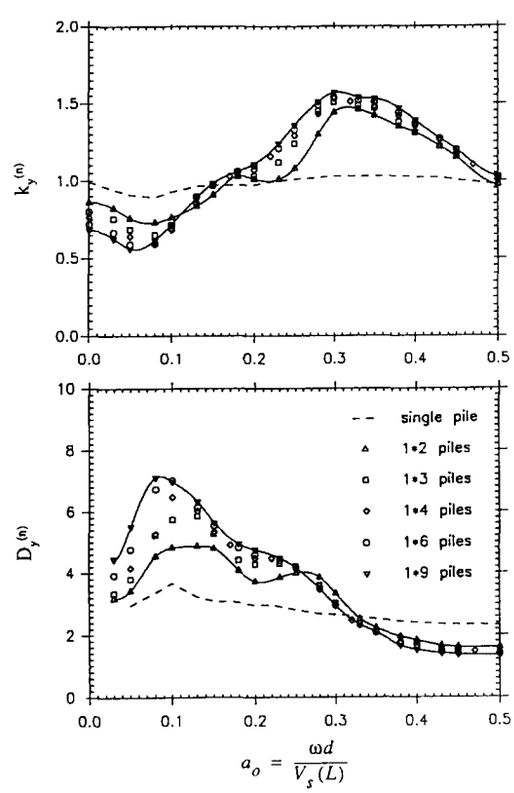

Fig. 23. Normalized horizontal dynamic stiffness and damping group factors of $1 \times n$ rigidly-capped pile groups in a nonhomogeneous half-space ($E_p/E_s(L) = 5000$, $L/d = 20$, $s/d = 5$, $\rho_s/\rho_p = 0{\cdot}7$, $\beta_s = 0{\cdot}05$ and $\nu_s = 0{\cdot}4$): effect of pile group configurations.

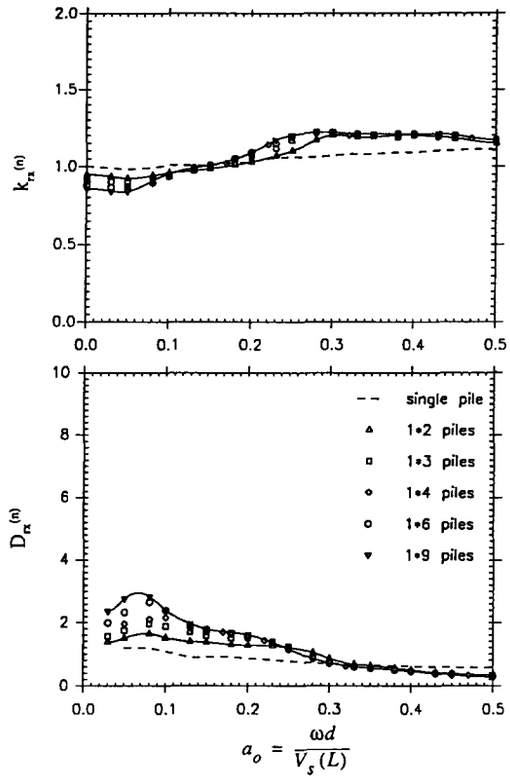

Fig. 24. Normalized rotational dynamic stiffness and damping group factors of $1 \times n$ rigidly-capped pile groups in a nonhomogeneous half-space ($E_p/E_s(L) = 5000$, $L/d = 20$, $s/d = 5$, $\rho_s/\rho_p = 0{\cdot}7$, $\beta_s = 0{\cdot}05$ and $\nu_s = 0{\cdot}4$): effect of pile group configurations.

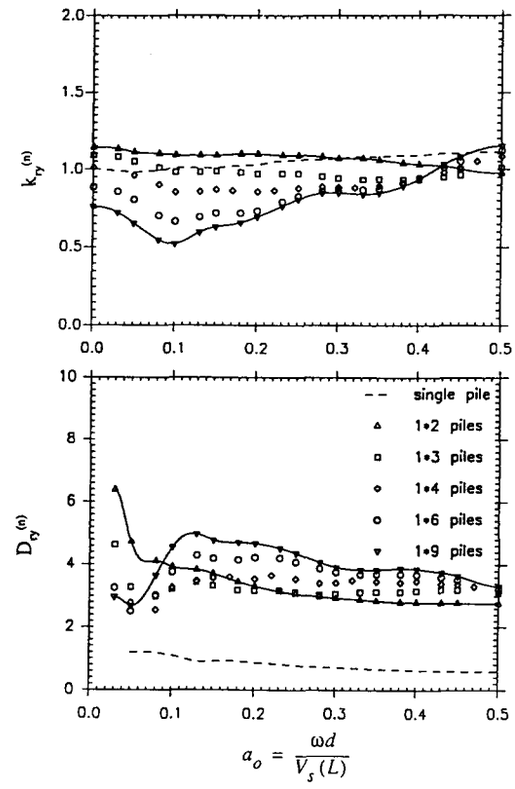

Fig. 25. Normalized rotational dynamic stiffness and damping group factors of $1 \times n$ rigidly-capped pile groups in a nonhomogeneous half-space ($E_p/E_s(L) = 5000$, $L/d = 20$, $s/d = 5$, $\rho_s/\rho_p = 0{\cdot}7$, $\beta_s = 0{\cdot}05$ and $\nu_s = 0{\cdot}4$): effect of pile group configurations.

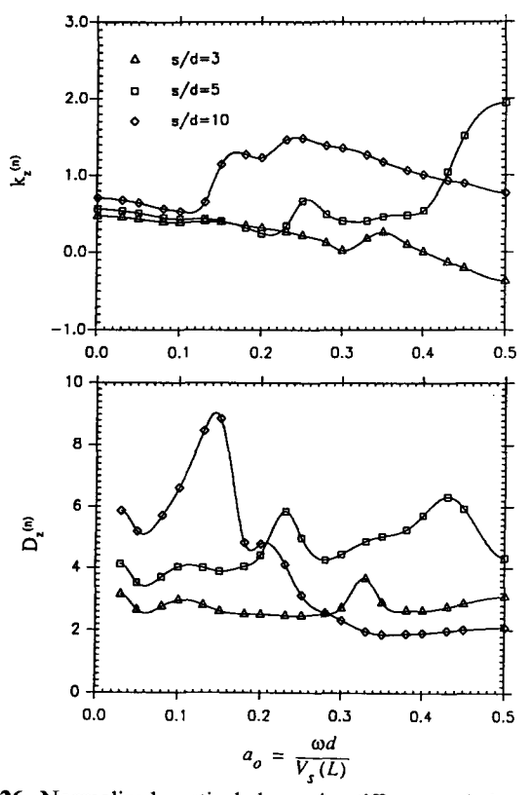

Fig. 26. Normalized vertical dynamic stiffness and damping group factors of 2×2 rigidly-capped pile groups in a nonhomogeneous half-space ($E_p/E_s(L) = 5000$, $L/d = 20$, $s/d = 5$, $\rho_s/\rho_p = 0{\cdot}7$, $\beta_s = 0{\cdot}05$ and $\nu_s = 0{\cdot}4$): effects of frequency and pile separation distance.

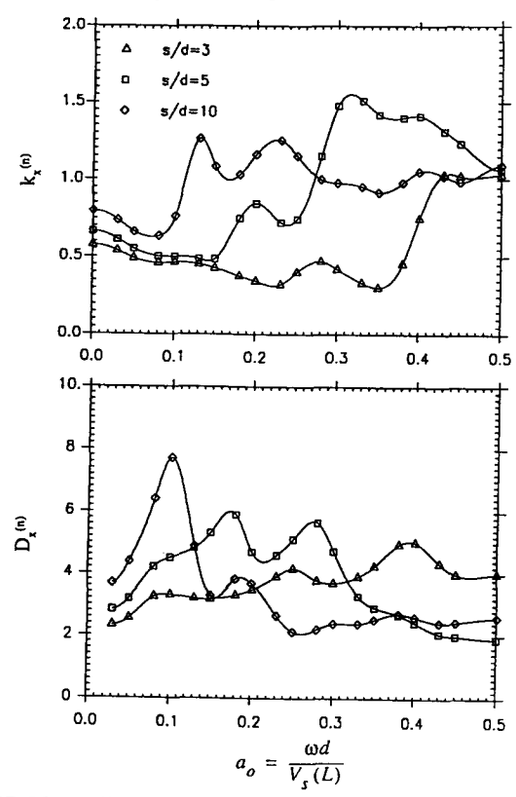

Fig. 27. Normalized horizontal dynamic stiffness and damping group factors of 2×2 rigidly-capped pile groups in a nonhomogeneous half-space ($E_p/E_s(L) = 5000$, $L/d = 20$, $s/d = 5$, $\rho_s/\rho_p = 0{\cdot}7$, $\beta_s = 0{\cdot}05$ and $\nu_s = 0{\cdot}4$): effects of frequency and pile separation distance.

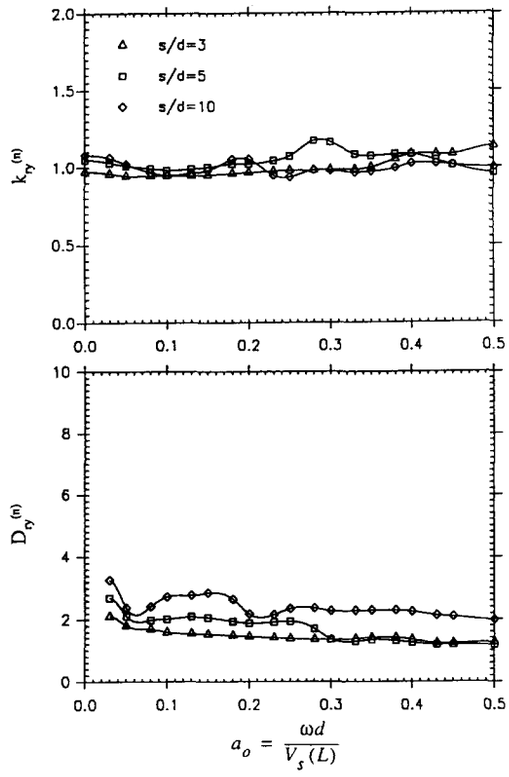

Fig. 28. Normalized rotational dynamic stiffness and damping group factors of 2×2 rigidly-capped pile groups in a nonhomogeneous half-space ($E_p/E_s(L) = 5000$, $L/d = 20$, $s/d = 5$, $\rho_s/\rho_p = 0{\cdot}7$, $\beta_s = 0{\cdot}05$ and $\nu_s = 0{\cdot}4$): effects of frequency and pile separation distance.

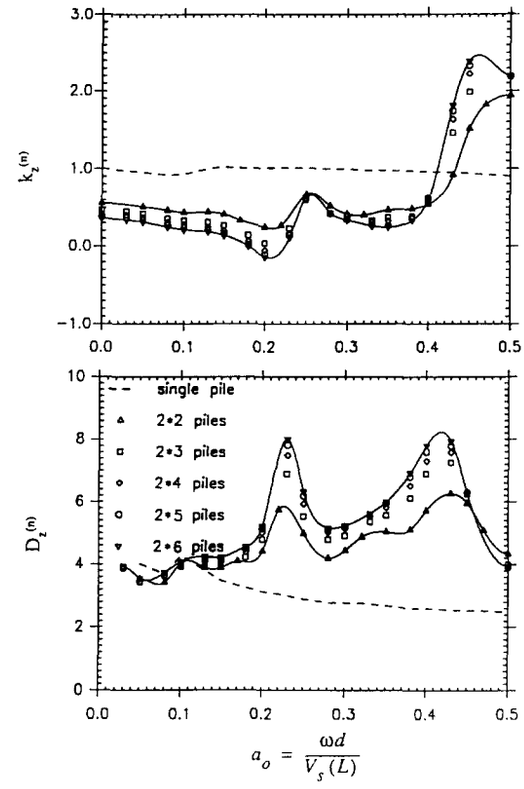

Fig. 29. Normalized vertical dynamic stiffness and damping group factors of $2 \times n$ rigidly-capped pile groups in a nonhomogeneous half-space ($E_p/E_s(L) = 5000$, $L/d = 20$, $s/d = 5$, $\rho_s/\rho_p = 0{\cdot}7$, $\beta_s = 0{\cdot}05$ and $\nu_s = 0{\cdot}4$): effect of pile group configurations.

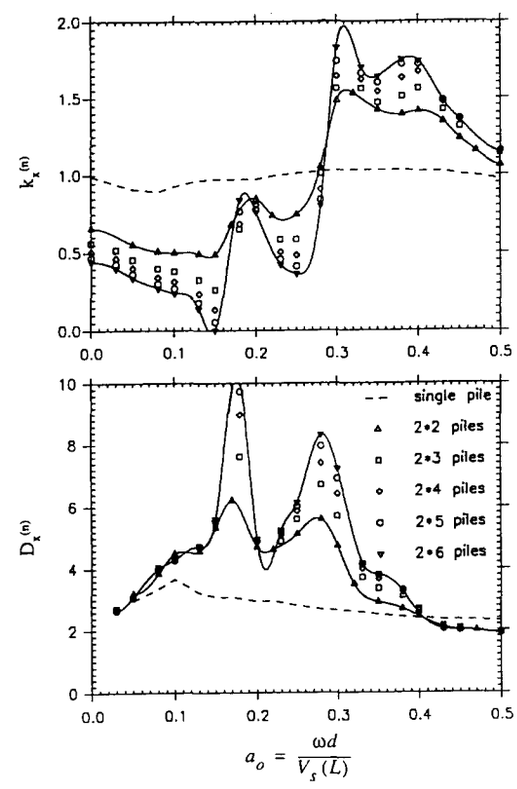

Fig. 30. Normalized horizontal dynamic stiffness and damping group factors of $2 \times n$ rigidly-capped pile groups in a nonhomogeneous half-space ($E_p/E_s(L) = 5000$, $L/d = 20$, $s/d = 5$, $\rho_s/\rho_p = 0{\cdot}7$, $\beta_s = 0{\cdot}05$ and $\nu_s = 0{\cdot}4$): effect of pile group configurations.

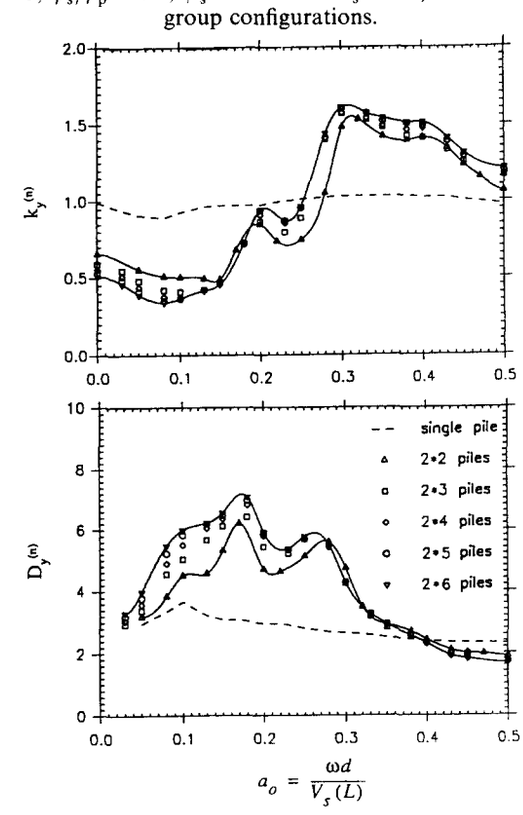

Fig. 31. Normalized horizontal dynamic stiffness and damping group factors of $2 \times n$ rigidly-capped pile groups in a nonhomogeneous half-space ($E_p/E_s(L) = 5000$, $L/d = 20$, $s/d = 5$, $\rho_s/\rho_p = 0{\cdot}7$, $\beta_s = 0{\cdot}05$ and $\nu_s = 0{\cdot}4$): effect of pile group configurations.

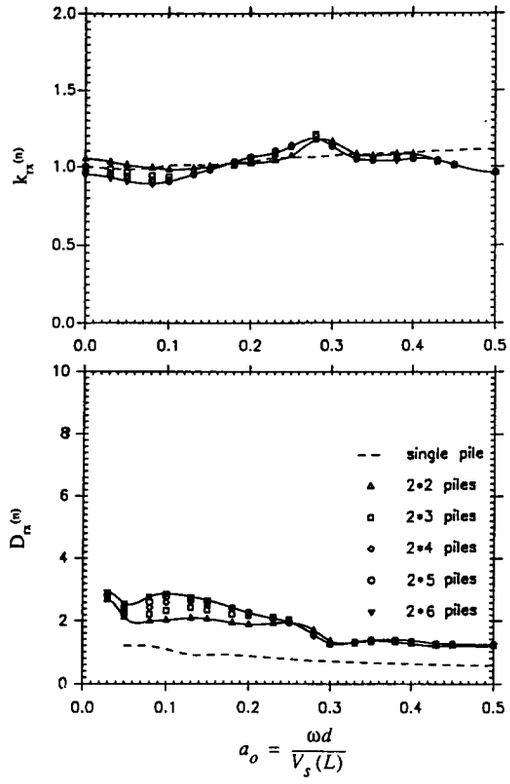

Fig. 32. Normalized rotational dynamic stiffness and damping group factors of $2 \times n$ rigidly-capped pile groups in a nonhomogeneous half-space ($E_p/E_s(L) = 5000$, $L/d = 20$, $s/d = 5$, $\rho_s/\rho_p = 0{\cdot}7$, $\beta_s = 0{\cdot}05$ and $\nu_s = 0{\cdot}4$): effect of pile group configurations.

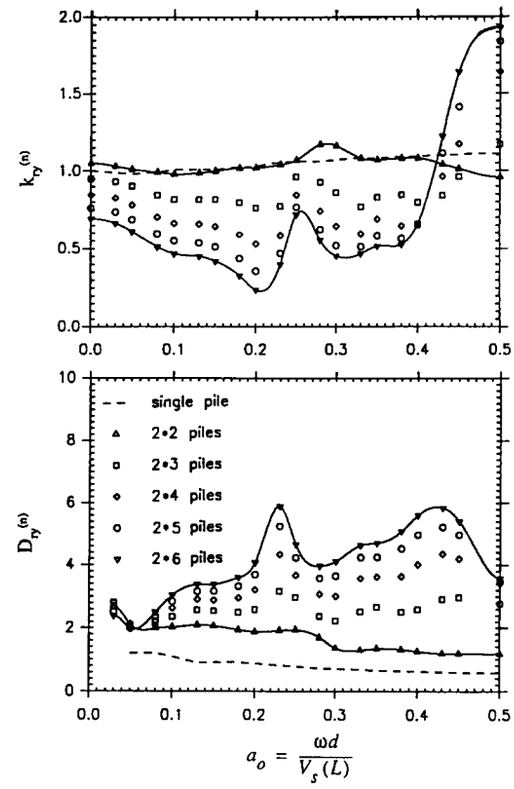

Fig. 33. Normalized rotational dynamic stiffness and damping group factors of $2 \times n$ rigidly-capped pile groups in a nonhomogeneous half-space ($E_p/E_s(L) = 5000$, $L/d = 20$, $s/d = 5$, $\rho_s/\rho_p = 0{\cdot}7$, $\beta_s = 0{\cdot}05$ and $\nu_s = 0{\cdot}4$): effect of pile group configurations.

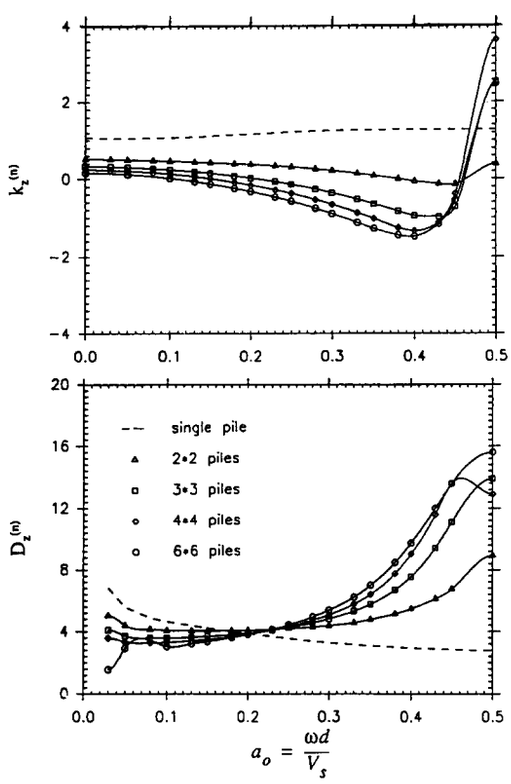

Fig. 34. Normalized vertical dynamic stiffness and damping group factors of $n \times n$ rigidly-capped pile groups in a homogeneous half-space ($E_p/E_s = 1000$, $L/d = 15$, $s/d = 5$, $\rho_s/\rho_p = 0{\cdot}7$, $\beta_s = 0{\cdot}05$ and $\nu_s = 0{\cdot}4$): effect of pile group configurations.

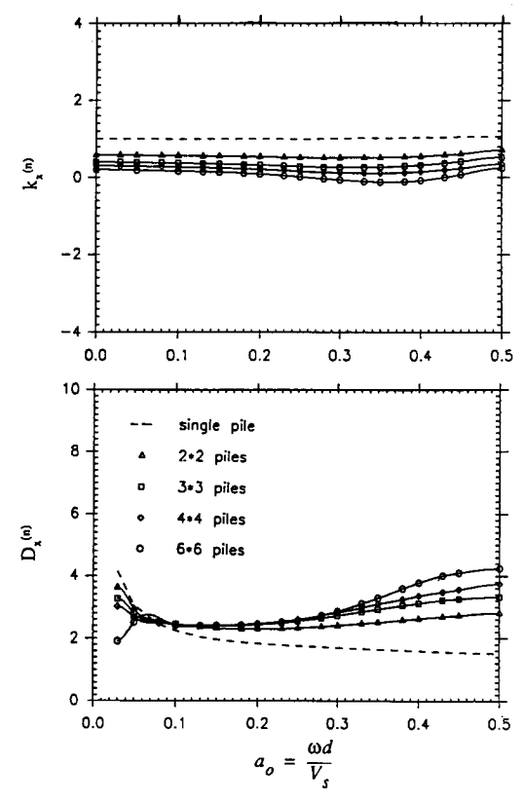

Fig. 35. Normalized horizontal dynamic stiffness and damping group factors of $n \times n$ rigidly-capped pile groups in a homogeneous half-space ($E_p/E_s = 1000$, $L/d = 15$, $s/d = 5$, $\rho_s/\rho_p = 0{\cdot}7$, $\beta_s = 0{\cdot}05$ and $\nu_s = 0{\cdot}4$): effect of pile group configurations.

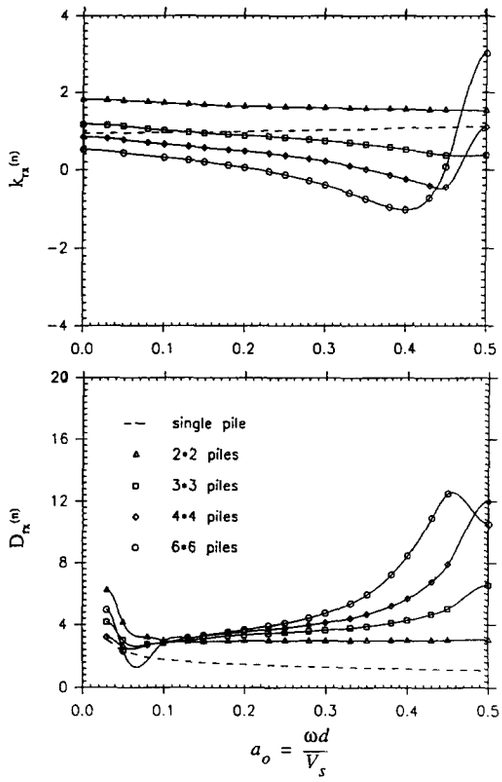

Fig. 36. Normalized rotational dynamic stiffness and damping group factors of $n \times n$ rigidly-capped pile groups in a homogeneous half-space ($E_p/E_s = 1000$, $L/d = 15$, $s/d = 5$, $\rho_s/\rho_p = 0{\cdot}7$, $\beta_s = 0{\cdot}05$ and $\nu_s = 0{\cdot}4$): effect of pile group configurations.

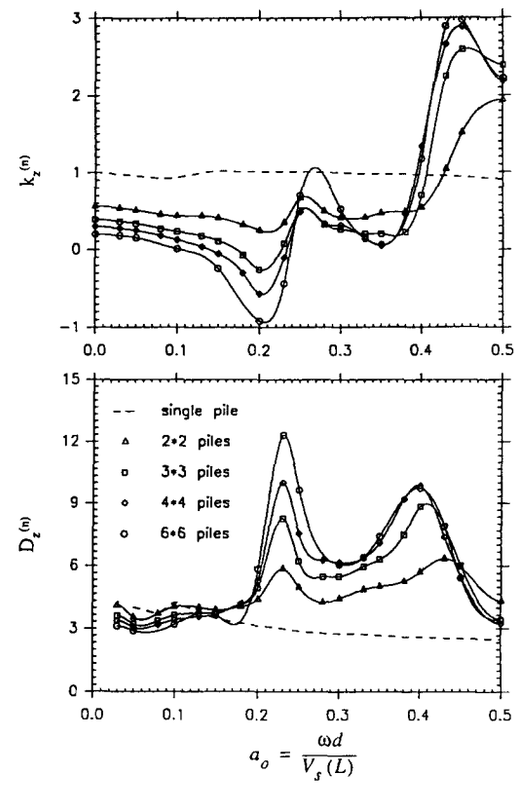

Fig. 37. Normalized vertical dynamic stiffness and damping group factors of $n \times n$ rigidly-capped pile groups in a nonhomogeneous half-space ($E_p/E_s(L) = 5000$, $L/d = 15$, $s/d = 5$, $\rho_s/\rho_p = 0{\cdot}7$, $\beta_s = 0{\cdot}05$ and $\nu_s = 0{\cdot}4$): effect of pile group configurations.

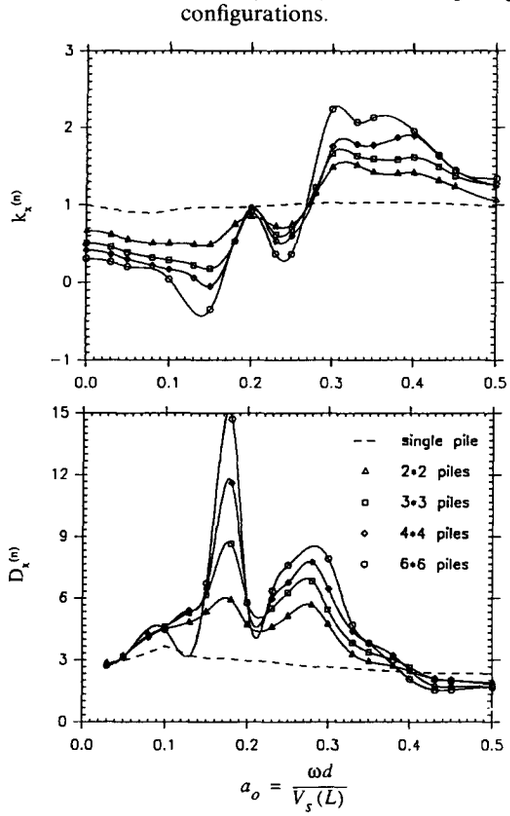

Fig. 38. Normalized horizontal dynamic stiffness and damping group factors of $n \times n$ rigidly-capped pile groups in a nonhomogeneous half-space ($E_p/E_s(L) = 5000$, $L/d = 15$, $s/d = 5$, $\rho_s/\rho_p = 0{\cdot}7$, $\beta_s = 0{\cdot}05$ and $\nu_s = 0{\cdot}4$): effect of pile group configurations.

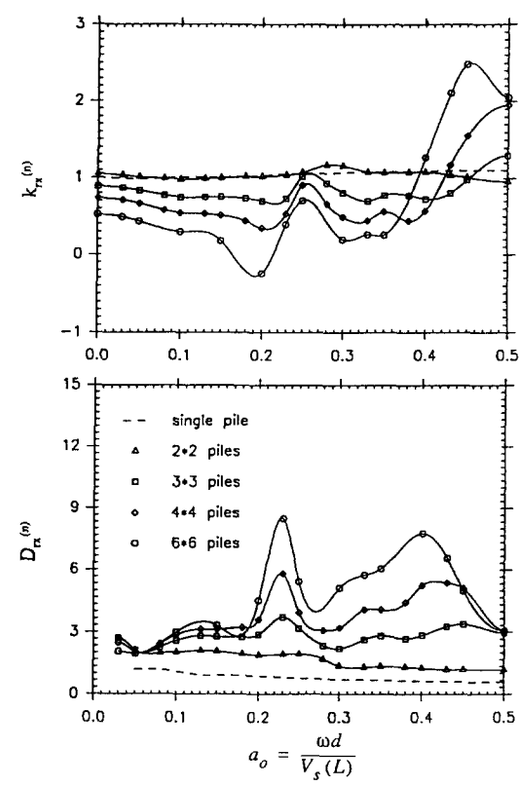

Fig. 39. Normalized rotational dynamic stiffness and damping group factors of $n \times n$ rigidly-capped pile groups in a nonhomogeneous half-space ($E_p/E_s(L) = 5000$, $L/d = 15$, $s/d = 5$, $\rho_s/\rho_p = 0{\cdot}7$, $\beta_s = 0{\cdot}05$ and $\nu_s = 0{\cdot}4$): effect of pile group configurations.

Table 2. Impedance functions of single piles: simplified[a] vs rigorous[a] ($E_p/E_s = 1000$, $L/d = 15$)
$\kappa = \bar{K} + i\omega C$

a_0	$\frac{\bar{K}_{x1}}{dE_s}$ ×5	$\frac{\bar{K}_{x2}}{dE_s}$ ×5	$\frac{C_{x1}}{dE_s}$ ×0·5	$\frac{C_{x2}}{dE_s}$ ×0·5	$\frac{\bar{K}_{z1}}{dE_s}$ ×50	$\frac{\bar{K}_{z2}}{dE_s}$ ×50	$\frac{C_{z1}}{dE_s}$ ×0·5	$\frac{C_{z2}}{dE_s}$ ×0·5	$\frac{\bar{K}_{rx1}}{d^3E_s}$ ×50	$\frac{\bar{K}_{rx2}}{d^3E_s}$ ×50	$\frac{C_{rx1}}{d^3E_s}$ ×0·5	$\frac{C_{rx2}}{d^3E_s}$ ×0·5
0·0		0·850	—	—		0·176	—	—		0·548	—	—
0·1		0·848	0·253	0·227		0·178	0·815	1·15		0·552	0·65	0·661
0·2		0·848	0·200	0·225		0·195	0·710	0·96		0·559	0·508	0·523
0·3		0·854	0·183	0·208		0·209	0·655	0·81		0·569	0·460	0·462
0·4		0·866	0·174	0·197		0·214	0·618	0·75		0·580	0·436	0·418
0·5	0·853	0·875	0·169	0·187	0·231	0·215	0·591	0·68	0·534	0·590	0·422	0·380
0·6		0·881	0·166	0·180		0·214	0·570	0·65		0·599	0·412	0·350
0·7		0·882	0·163	0·175		0·210	0·553	0·62		0·606	0·405	0·329
0·8		0·880	0·161	0·170		0·204	0·538	0·61		0·612	0·400	0·313
0·9		0·875	0·160	0·166		0·196	0·525	0·60		0·618	0·396	0·300
1·0		0·865	0·158	0·163		0·185	0·515	0·59		0·624	0·393	0·290

[a] See Refs 19 and 25.

rigorous) dynamic interaction factors; and (c) direct numerical solutions.

In principle the last method is more rigorous, but a sophisticated computer code is usually needed. The first and second methods are conceptually simple. They use the dynamic impedances of single piles as the basis and account for the group effect by means of interaction factors (static or dynamic). Closed-form expressions for the impedances of single piles in three idealized soil deposits, for all modes of vibration, have been developed by Gazetas.[19]

Table 2 compares the dynamic impedances of single piles computed with these simple expressions with those computed with the rigorous solution of Kaynia & Kausel.[17] The stiffness coefficient in the simplified method is taken to be independent of frequency. This was confirmed as a good approximation. Overall the comparison is quite good. The 'rigorous' stiffness is practically independent of frequency and the damping does not rely on frequency at intermediate and high a_0.

The use of static interaction factors is still popular in current practice. The group stiffness and damping are estimated from the static interaction factor (in displacement or rotation) from Poulos.[20–22] This approach cannot predict properly the dynamic response of pile groups, except perhaps at very low frequencies of oscillation. The dynamic interaction factors are complex, quite different from static ones, and both real and imaginary parts can be negative at certain frequencies, which means that at such frequencies the displacements of pile groups may be less than those of single piles subject to the same average pile loading. Therefore the dynamic group 'efficiency' may far exceed unity, whereas the static 'efficiency' is well below unity, especially with a large number of piles.

Therefore, the dynamic-interaction-factor approach is the only one that can be recommended in engineering practice. The dynamic interaction factors are available in dimensionless charts for two typical soil profiles (see Ref. 3). Also, they are available in simple analytical

Table 3. Vertical impedance functions[a] of 2 × 2 piles ($E_p/E_s = 1000$, $L/d = 15$, $\beta_s = 0.05$, $\nu_s = 0.4$)
$\kappa = \bar{K} + i\omega C$

a_0	$s/d = 2$						$s/d = 5$						$s/d = 10$					
	$\frac{\bar{K}_{z1}}{dE_s}$ ×50	$\frac{\bar{K}_{z2}}{dE_s}$ ×50	$\frac{\bar{K}_{z3}}{dE_s}$ ×50	$\frac{C_{z1}}{dE_s}$ ×5	$\frac{C_{z2}}{dE_s}$ ×5	$\frac{C_{z3}}{dE_s}$ ×5	$\frac{\bar{K}_{z1}}{dE_s}$ ×50	$\frac{\bar{K}_{z2}}{dE_s}$ ×50	$\frac{\bar{K}_{z3}}{dE_s}$ ×50	$\frac{C_{z1}}{dE_s}$ ×5	$\frac{C_{z2}}{dE_s}$ ×5	$\frac{C_{z3}}{dE_s}$ ×5	$\frac{\bar{K}_{z1}}{dE_s}$ ×50	$\frac{\bar{K}_{z2}}{dE_s}$ ×50	$\frac{\bar{K}_{z3}}{dE_s}$ ×50	$\frac{C_{z1}}{dE_s}$ ×5	$\frac{C_{z2}}{dE_s}$ ×5	$\frac{C_{z3}}{dE_s}$ ×5
0·0		0·267	0·270	—	—	—		0·348	0·350	—	—	—		0·440	0·436	—	—	—
0·1		0·250	0·256		0·250	0·251		0·310	0·312		0·401	0·413		0·395	0·393		0·650	0·661
0·2		0·252	0·253		0·221	0·226		0·268	0·261		0·412	0·423		0·563	0·607		0·808	0·895
0·3		0·231	0·231		0·204	0·206		0·160	0·165		0·432	0·449		1·619	1·590		0·486	0·290
0·4		0·175	0·176		0·191	0·194		0·016	0·016		0·559	0·560		1·101	1·030		0·160	0·154
0·5	0·330	0·093	0·094	0·101	0·190	0·189	0·444	0·462	0·461	0·136	0·900	0·899	0·553	0·803	0·794	0·169	0·178	0·183
0·6		−0·015	−0·014		0·185	0·188		2·946	2·940		0·454	0·462		0·670	0·661		0·208	0·214
0·7		−0·200	−0·154		0·186	0·191		2·014	2·010		0·147	0·152		0·587	0·580		0·238	0·241
0·8		−0·460	−0·336		0·183	0·185		1·490	1·450		0·135	0·130		0·545	0·540		0·275	0·270
0·9		−0·720	−0·570		0·186	0·186		1·126	1·120		0·144	0·137		0·661	0·667		0·342	0·308
1·0		−1·200	−0·877		0·186	0·190		0·881	0·885		0·144	0·148		1·180	1·120		0·294	0·291

[a] Subscripts: 1, using static interaction factors; 2, using dynamic interaction factors; 3, using rigorous method.

Table 4. Vertical impedance functions[a] of 3 × 3 piles ($E_p/E_s = 1000$, $L/d = 15$, $\beta_s = 0{\cdot}05$, $\nu_s = 0{\cdot}4$)
$\kappa = \bar{K} + i\omega C$

a_0	$s/d = 2$						$s/d = 5$						$s/d = 10$					
	$\frac{\bar{K}_{z1}}{dE_s}$ ×50	$\frac{\bar{K}_{z2}}{dE_s}$ ×50	$\frac{\bar{K}_{z3}}{dE_s}$ ×50	$\frac{C_{z1}}{dE_s}$ ×5	$\frac{C_{z2}}{dE_s}$ ×5	$\frac{C_{z3}}{dE_s}$ ×5	$\frac{\bar{K}_{z1}}{dE_s}$ ×50	$\frac{\bar{K}_{z2}}{dE_s}$ ×50	$\frac{\bar{K}_{z3}}{dE_s}$ ×50	$\frac{C_{z1}}{dE_s}$ ×5	$\frac{C_{z2}}{dE_s}$ ×5	$\frac{C_{z3}}{dE_s}$ ×5	$\frac{\bar{K}_{z1}}{dE_s}$ ×50	$\frac{\bar{K}_{z2}}{dE_s}$ ×50	$\frac{\bar{K}_{z3}}{dE_s}$ ×50	$\frac{C_{z1}}{dE_s}$ ×5	$\frac{C_{z2}}{dE_s}$ ×5	$\frac{C_{z3}}{dE_s}$ ×5
0·0		0·348	0·347	—	—	—		0·495	0·506	—	—	—		0·634	0·705	—	—	—
0·1		0·312	0·305		0·388	0·401		0·371	0·367		0·815	0·825		0·490	0·485		1·785	1·775
0·2		0·251	0·247		0·380	0·375		0·055	0·060		0·883	0·903		1·584	2·29		2·469	2·778
0·3		0·132	0·135		0·348	0·354		−0·501	−0·494		1·133	1·131		3·643	3·120		0·729	0·588
0·4		−0·048	−0·052		0·339	0·344		−1·209	−1·210		1·808	1·810		2·695	2·770		0·585	0·382
0·5	0·425	−0·320	−0·309	0·114	0·344	0·344	0·642	4·830	4·780	0·172	2·987	2·892	0·892	1·820	1·780	0·240	0·299	0·293
0·6		−0·642	−0·635		0·341	0·345		7·603	6·270		0·650	0·646		1·114	1·140		0·440	0·439
0·7		−1·223	−1·040		0·344	0·349		4·251	4·370		0·381	0·386		1·002	1·140		0·631	0·625
0·8		−1·865	−1·560		0·342	0·355		3·546	3·730		0·364	0·359		1·535	1·470		0·592	0·585
0·9		−2·693	−2·210		0·292	0·361		3·210	3·340		0·258	0·254		0·930	0·925		0·658	0·666
1·0		−4·118	−3·040		0·201	0·367		2·243	2·300		0·225	0·216		2·780	2·870		0·837	0·779

[a] Subscripts: 1, using static interaction factors; 2, using dynamic interaction factors; 3, using rigorous method.

forms for homogeneous and nonhomogeneous soils. For example, for a homogeneous soil profile:

For vertical oscillation,

$$\alpha_v \approx \frac{1}{\sqrt{2}}\left(\frac{s}{d}\right)^{-1/2}\exp\left(\frac{-\beta_s\omega s}{V_s}\right)\exp\left(\frac{-i\omega s}{V_s}\right) \qquad (12)$$

For horizontal oscillation,

$$\alpha_h(0^\circ) \approx \frac{1}{\sqrt{2}}\left(\frac{s}{d}\right)^{-1/2}\exp\left(\frac{-\beta_s\omega s}{V_{La}}\right)\exp\left(\frac{-i\omega s}{V_{La}}\right) \qquad (13)$$

$$\alpha_h(90^\circ) \approx \tfrac{3}{4}\alpha_v \qquad (14)$$

$$\alpha_h(0^\circ) \approx \alpha_h(0^\circ)\cos^2\theta + \alpha_h(90^\circ)\sin^2\theta \qquad (15)$$

The group stiffness and damping are evaluated in a similar way to the static case. The impedances of 2 × 2 and 3 × 3 pile groups predicted from static and dynamic interaction factors are compared with the rigorous numerical solutions in Tables 3, 4 and 5.

In Tables 3 and 4 the vertical group stiffness and damping coefficients from the dynamic-interaction-factor method compare very well with the rigorous numerical solution. Even some detailed trends are successfully predicted. The difference between these two methods is generally within 10%. The reason why such a greatly simplified solution can provide practically accurate results to the complicated boundary-value problem is that the key physical feature of cylindrical shear wave interference is adequately captured. Table 5 presents the results of horizontal impedances for 2 × 2 pile groups. The predictions by the dynamic-interaction-factor approach is not fully satisfactory, particularly near the peaks. This is probably due to the assumption of simultaneous emission of waves from different depths along each of the piles, which is a crucial assumption in the model of Dobry & Gazetas[23] and Makris & Gazetas.[7] The flexural waves may propagate down the

Table 5. Horizontal impedance functions[a] of 2 × 2 piles ($E_p/E_s = 1000$, $L/d = 15$, $\beta_s = 0.05$, $\nu_s = 0.4$)
$\kappa = \bar{K} + i\omega C$

a_0	$s/d = 2$						$s/d = 5$						$s/d = 10$					
	$\frac{\bar{K}_{x1}}{dE_s}$ ×50	$\frac{\bar{K}_{x2}}{dE_s}$ ×50	$\frac{\bar{K}_{x3}}{dE_s}$ ×50	$\frac{C_{x1}}{dE_s}$ ×0·5	$\frac{C_{x2}}{dE_s}$ ×0·5	$\frac{C_{x3}}{dE_s}$ ×0·5	$\frac{\bar{K}_{x1}}{dE_s}$ ×50	$\frac{\bar{K}_{x2}}{dE_s}$ ×50	$\frac{\bar{K}_{x3}}{dE_s}$ ×50	$\frac{C_{x1}}{dE_s}$ ×0·5	$\frac{C_{x2}}{dE_s}$ ×0·5	$\frac{C_{x3}}{dE_s}$ ×0·5	$\frac{\bar{K}_{x1}}{dE_s}$ ×50	$\frac{\bar{K}_{x2}}{dE_s}$ ×50	$\frac{\bar{K}_{x3}}{dE_s}$ ×50	$\frac{C_{x1}}{dE_s}$ ×0·5	$\frac{C_{x2}}{dE_s}$ ×0·5	$\frac{C_{x3}}{dE_s}$ ×0·5
0·0		0·143	0·155	—	—	—		0·170	0·202	—	—	—		0·238	0·246	—		—
0·1		0·136	0·152		0·634	0·767		0·168	0·198		0·121	0·124		0·221	0·252		0·182	0·176
0·2		0·133	0·146		0·601	0·676		0·161	0·190		0·104	0·116		0·238	0·288		0·187	0·165
0·3		0·119	0·146		0·600	0·660		0·160	0·184		0·113	0·120		0·395	0·390		0·165	0·140
0·4		0·109	0·134		0·600	0·652		0·142	0·196		0·120	0·128		0·459	0·439		0·102	0·183
0·5	0·157	0·085	0·125	0·327	0·590	0·641	0·220	0·147	0·235	0·458	0·143	0·136	0·270	0·425	0·391	0·560	0·064	0·062
0·6		0·068	0·113		0·580	0·631		0·255	0·334		0·167	0·143		0·408	0·348		0·063	0·063
0·7		0·051	0·097		0·59	0·629		0·391	0·518		0·146	0·124		0·374	0·335		0·062	0·067
0·8		0·027	0·076		0·600	0·629		0·593	0·592		0·123	0·082		0·357	0·327		0·065	0·070
0·9		−0·041	−0·051		0·610	0·634		0·541	0·523		0·097	0·058		0·348	0·338		0·071	0·073
1·0		−0·088	0·020		0·614	0·641		0·510	0·442		0·074	0·052		0·384	0·385		0·068	0·073

[a] Subscripts: 1, using static interaction factors; 2, using dynamic interaction factors; 3, using rigorous method.

laterally loaded pile at a finite apparent phase velocity, rendering the assumption of simultaneous arrival of these waves not strictly valid. Consequently, the waves that are arriving, even in homogeneous soil, have different phases along this pile, which is not accounted for in the simple model.

The group impedances predicted by using static interaction factors are close to those from the numerical solutions only at very low frequencies. At intermediate and high frequencies use of static interaction factors leads to erroneous results. In fact, it appears that it is better to ignore pile-to-pile interaction altogether than to use static interaction factors — a conclusion echoed by Novak.[24]

CONCLUSION

A systematic parametric study has been presented on the effect of pile group configuration upon dynamic impedances of piles embedded in homogeneous as well as in inhomogeneous soils. It has been shown that the cross-interaction between piles in different rows controls the dynamic response of a 'rectangular' pile group; increasing the number of piles in a line group has very little effect on the dynamic stiffness and damping factors.

The comparative study of two simple methods and the rigorous numerical solution has been conducted for 2×2 and 3×3 pile groups. It has been demonstrated that the predictions by the static-interaction-factor method are acceptable only for static and low-frequency cases; they may be very conservative or very unsafe at higher frequencies. The dynamic-interaction-factor approach successfully predicts the dynamic response of pile groups in most cases.

REFERENCES

1. Fan, K. Seismic response of pile foundations evaluated through case histories. Ph.D. dissertation, State University of New York, Buffalo, 1992.
2. Fan, K., Gazetas, G., Kaynia, A., Kausel, E. & Ahmad, S. Kinematic seismic response of single piles and pile groups. *J. Geotech. Eng., ASCE*, 1991, **117**(12), 1860–79.
3. Gazetas, G., Fan, K., Kaynia, A. & Kausel, E. Dynamic interaction factors for floating pile groups. *J. Geotech. Engng Div., ASCE*, 1991, **117**(10), 1531–48.
4. Gazetas, G. Seismic response of end-bearing single piles. *Soil Dynamics Earthq. Engng*, 1984, **3**(2), 82–93.
5. Gazetas, G., Fan, K., Tazoh, T., Shimizu, K., Kavvadas, M. & Makris, N. *et al.* Seismic pile-group–structure interaction. Piles under Dynamic Loads, ed. S. Prakash, ASCE, New York City, NY, 1992, 56–94.
6. Kavvadas, M. & Gazetas, G. Kinematic seismic response and bending of free-head piles in layered soil. *Geotechnique*, 1993, **43**(2), 207–22.
7. Makris, N. & Gazetas, G. Dynamic pile–soil–pile interaction. Part II: Lateral and seismic response. *Earthq. Engng Struct. Dynamics*, 1992, **21**(2), 145–62.
8. Novak, M. Dynamic stiffness and damping of piles. *Canadian Geotech. J.*, 1974, **11**(4), 574–98.
9. Novak, M. Experiments with shallow and deep foundations. *Vibration Problems in Geotechnical Engineering*, ed. G. Gazetas & E.T. Selig. ASCE, 1985, pp. 1–26.
10. Novak, M., Nogami, T. & Aboul-Ellq, F. Dynamic soil reactions for plane strain case. *J. Eng. Mech. Div.*, ASCE, 1978, **104**, No. EM4, pp. 953–9.
11. Gazetas, G. & Dobry, R. Horizontal response of piles in layered soils. *J. Geotech. Engng Div., ASCE*, 1984, **110**(1), 20–40.
12. Gazetas, G. Simple physical methods for foundation impedances. *Dynamic Behavior of Foundations and Buried Structures*. Elsevier Applied Science, London, 1987, pp. 45–93.
13. Wolf, J.P. & Meek, J.W. Cone models for a pile foundation. *Piles Under Dynamic Loads*, ed. S. Prakash. ASCE, 1992, pp. 94–113.
14. Liou, D.D. & Penzien, J. Seismic analysis of an offshore structure supported on pile foundations. Report No. EERC77-25, University of California, Berkeley, 1977.
15. Roesset, J.M. & Angelides, D. Dynamic stiffness of piles. *Numerical Methods in Offshore Piling*. CE, London, 1980, pp. 75–81.
16. Kagawa, T. & Kraft, L.M. Lateral load-deflection relationship of piles subjected to dynamic loadings. *Soils and Foundations*, 1980, **20**(4), 19–36.
17. Kaynia, A.M. & Kausel, E. Dynamic behavior of pile groups. *Proc. 2nd International Conf. on Num. Meth. in Offshore Piling*, Prustin, Texas, 1992, 509–32.
18. Tazoh, T., Shimizu, K. & Wakahara, T. Seismic observations and analysis of grouped piles. *Shimizu Technica Research Bulletin*, No. 7, 1988.
19. Gazetas, G. Foundation vibrations. *Foundation Engineering Handbook*, 2nd edn, ed. Y. Fang, Van Nostrand Reinhold, New York, 1991, pp. 553–93.
20. Poulos, H.G. Analysis of the settlement of pile groups. *Geotechnique*, 1968, **19**, 449–71.
21. Poulos, H.G. Behavior of laterally-loaded piles: II, Pile groups. *J. Soil Mech. & Foundn Div.*, ASCE, 1971, **97**, No. SM5, 733–51.
22. Poulos, G.G. & Davis, E.H. *Pile Foundation Analysis and Design*. John Wiley and Sons, New York, 1980.
23. Dobry, R. & Gazetas, G. Simple method for dynamic stiffness and damping of floating pile groups. *Geotechnique*, 1988, **38**(4), 557–74.
24. Novak, M. Piles under dynamic loads: State of the art. *Proc. 2nd Int. Conf. on Recent Advances in Geotech. Earthq. Engng. & Soil Dynamics*, III. Univ. of Missouri-Rolla, 1991, p. 43.